

Multiscale scanning in inverse problems

KATHARINA PROKSCH¹

`kproksc@uni-goettingen.de`

Institute for Mathematical Stochastics, University of Göttingen

FRANK WERNER

`frank.werner@mpibpc.mpg.de`

Max Planck Institute for Biophysical Chemistry, Göttingen, Germany

AXEL MUNK

`munk@math.uni-goettingen.de`

Institute for Mathematical Stochastics, University of Göttingen

and

Felix Bernstein Institute for Mathematical Statistics in the Bioscience,
University of Göttingen

and

Max Planck Institute for Biophysical Chemistry, Göttingen, Germany

In this paper we propose a multiscale scanning method to determine active components of a quantity f w.r.t. a dictionary \mathcal{U} from observations Y in an inverse regression model $Y = Tf + \xi$ with operator T and general random error ξ . To this end, we provide uniform confidence statements for the coefficients $\langle \varphi, f \rangle$, $\varphi \in \mathcal{U}$, under the assumption that $(T^*)^{-1}(\mathcal{U})$ is of wavelet-type. Based on this we obtain a decision rule that allows to identify the active components of \mathcal{U} , i.e. $\langle f, \varphi \rangle \neq 0$, $\varphi \in \mathcal{U}$, at controlled, family-wise error rate. Our results rely on a Gaussian approximation of the underlying multiscale statistic with a novel scale penalty adapted to the ill-posedness of the problem. The important special case of deconvolution is discussed in detail. Further, the pure regression case, when $T = \text{id}$ and the dictionary consists of moving windows of various sizes (scales), is included, generalizing previous results for this setting. Simulations support our theory and we illustrate the potential of the method as an inferential tool for imaging. As a particular application we discuss super-resolution microscopy and analyze experimental STED data to locate single DNA origami.

Keywords: multiscale analysis, scan statistic, ill-posed problem, deconvolution, super-resolution

AMS classification numbers: Primary 62G10, Secondary 62G15, 62G20, 62G32.

1 Introduction

Suppose we have access to observations $Y_{\mathbf{j}}$ which are linked to an unknown quantity $f \in \mathbb{H}_1$ via the inverse regression model

$$Y_{\mathbf{j}} = Tf(\mathbf{x}_{\mathbf{j}}) + \xi_{\mathbf{j}}, \quad \mathbf{j} \in I_n := \{1, \dots, n\}^d, \quad d \in \mathbb{N}. \quad (1)$$

Here, $T : \mathbb{H}_1 \rightarrow \mathbb{H}_2 \subset \mathbf{L}^2[0, 1]^d$ is a bounded linear operator, \mathbb{H}_1 and \mathbb{H}_2 denote proper Hilbert spaces, and the $\mathbf{x}_{\mathbf{j}}$, $\mathbf{j} \in I_n$, denote sampling-points in the d -cube $[0, 1]^d$. Concerning the noise we assume that $\xi_{\mathbf{j}}$, $\mathbf{j} \in I_n$, are independent, centered but not necessarily identically distributed random variables. Here and throughout the paper, bold print letters and numbers denote vectors and multi-indices, whereas scalars are printed in regular type face.

¹Corresponding author

Models of the kind (1) underly a plenitude of applied problems varying from astrophysics and tomography to cell biology, see, e.g. (O’Sullivan, 1986; Bertero et al., 2009), and have received considerable interest in the statistical literature. Much of research targets (regularized) estimation of f and associated theory, see, e.g. (Cavalier, 2011) or (Johnstone and Paul, 2014) for recent topical surveys. An early approach for estimation is based on a singular value decomposition (SVD) of the operator, where f is expanded in a series of eigenfunctions of T^*T , see, e.g. (Mair and Ruymgaart, 1996; Johnstone et al., 2004; Cavalier and Golubev, 2006; Bissantz et al., 2007; Kerkycharian et al., 2010; Albani et al., 2016). Given a proper choice of the regularization parameter, SVD-based estimators are well-known to be minimax optimal (Johnstone and Silverman, 1991). Adaptive estimation in this context was studied, e.g. by Goldenshluger (1999); Tsybakov (2000); Cavalier et al. (2003); Chernousova and Golubev (2014). Since in SVD-based estimation the basis for the expansion is entirely defined by the operator, as an alternative, wavelet-based methods which incorporate the properties of the function of interest have also been frequently employed. Examples are wavelet-vaguelette methods (WVM, Donoho (1995)) and vaguelette-wavelet methods (VWM, Abramovich and Silverman (1998)), where f and Kf are expanded in a wavelet and vaguelette or vaguelette and wavelet basis, respectively, and the coefficients are estimated by proper thresholding. This allows for a natural adaptation to the local smoothness of the unknown function, see e.g. (Cavalier and Tsybakov, 2002). Related to this, Cohen et al. (2004) proposed an adaptive estimator based on a combination of linear Galerkin projection methods and adaptive wavelet thresholding. Besides of these selective references a vast amount of work has been devoted to recovery of f during the last decades and the common ground of all these works is that the ill-posedness of an inverse problem usually only gives poor rates for estimation and makes full recovery of f a very difficult problem in general (in the setup of (1) see, e.g. (Willer, 2009) or for deconvolution, see, e.g., the monograph by Meister (2009) and the references given there).

However, in many applications, only certain properties or aspects of the function f are of interest and a full, precise reconstruction is not necessary any more. Examples of practical relevance are the detection and localization of "hot spots" in astrophysical image analysis (Friedenberg and Genovese, 2013), non-destructive testing (Kazantsev et al., 2002), and image deformation in microscopy (Bissantz et al., 2009), to mention a few. For a theoretical account in deconvolution see (Butucea and Comte, 2009). In a similar spirit, the detection of certain geometric shapes in image analysis has been studied by Genovese et al. (2012), but the authors do not take into account the underlying inverse problem. All these issues can be treated by means of statistical testing, presumably a simpler task than estimation.

In contrast to estimation, hypothesis testing in inverse problems has been investigated much less, early references are (Butucea, 2007; Holzmann et al., 2007). Ingster et al. (2012) treat the problem of testing $f = 0$ against $f \in \Theta_q(r)$ where $\Theta_q(r)$ is a suitable smoothness class restricted to $\|f\| \geq r$ by means of the classical minimax testing approach (see e.g. the series of papers by Ingster (1993)). Also Laurent et al. (2011, 2012) follow this path and investigate the differences and commonalities of testing in the image space ($Tf = 0$) and the preimage space ($f = 0$). The authors prove that in several situations it does not matter if first f is approximately reconstructed using an SVD-based regularization method and then tested to be 0, or if Tf is directly tested to be 0, see also Holzmann et al. (2007) for a similar observation. More precisely, minimax testing procedures for one of these problems are also minimax for the rephrased problem and the asymptotic detection boundary for both testing problems coincides. For related results in the multivariate setting or for more general regularization schemes see (Ingster et al., 2014; Marteau and Mathé, 2014). In contrast to the problem treated here, in all these studies only "global" features of the full signal are investigated, such as testing that the full signal is zero, and no simultaneous inference on sub-structures of the signal is targeted which is a much more challenging task and will be the topic of this paper.

Finding relevant sub-structures, such as the detection of regions of activity is of "scanning-type", which means that it can be reformulated as a (multiple) testing problem and a scanning-type procedure can be employed. A scan statistic is usually defined as the maximal value of a suitable family of test statistics S , evaluated at each element of a set of scanning windows. To be precise, if $S(Y, i)$ denotes the local test statistic evaluated at scanning window i , $i \in \mathcal{I}$, the corresponding

scan statistic is defined by

$$\mathcal{S}(Y) := \max_{i \in \mathcal{I}} S(Y, i). \quad (2)$$

Locally, for each fixed $i \in \mathcal{I}$, the tests are evaluated and compared to the (approximated) critical values of the maximum (2). Due to their wide range of applicability, scan statistics have received much attention in the literature over the past decades, e.g. in one-dimensional change point problems, see (Siegmund and Yakir, 2000) for an early reference and the monograph by Glaz et al. (2001) for a topical overview. In the context of one-dimensional segment detection Frick et al. (2014) defined a scan statistic that attains optimal asymptotic detection power at all scales, whereas the methods of Cai et al. (2012); Cai and Yuan (2014) attain optimal detection rates for sparse signals. The higher order criticism developed by Donoho and Jin (2004) can be viewed as a general scan statistic over a range of nominal levels, not necessarily linked to spatial structure. Walther (2010) considers the two dimensional problem of detecting spatial clusters in the Bernoulli model by scanning with rectangular windows of varying sizes, see also (Kablichko, 2011; Sharpnack and Arias-Castro, 2016) for results in a Gaussian setting. In a similar spirit, scan statistics have been employed in the context of multiscale inference about higher order qualitative characteristics such as modes of a one-dimensional density, see (Dümbgen and Walther, 2008; Rufibach and Walther, 2010). Finally, the family-wise error control provided by the maximum in (2) can be relaxed to relative measures of false positives, see, e.g. (Li et al., 2016) for segment detection, (Sun et al., 2015) for spatial scanning or (Zhang et al., 2016) for scanning of Poisson random fields which arise from DNA sequencing. In all these works, the scanning is performed by a system of properly-shaped scanning windows, well suited for regression, i.e. when $T = \text{id}$ in (1). Most similar in spirit to our work is (Arias-Castro et al., 2005), where a scanning procedure based on a multiscale dictionary of beamlets is proposed, that allows to detect line segments hidden in a noisy image, however, not in an inverse regression context. Schmidt-Hieber et al. (2013) infer on shape characteristics of a density in deconvolution, which is, however, restricted to the one-dimensional case.

Our contribution In this paper, we consider a general approach which is required for the treatment of inverse problems as in (1), denoted as **Multiscale Inverse Scanning Test** (MISCAT). The suggested method infers active components of f , i.e. detects "hot-spots" $|\langle f, \varphi_i \rangle| > 0$ with respect to a properly chosen dictionary $\mathcal{U} = \{\varphi_i\}_{i \in \{1, \dots, N\}} \subset \mathbb{H}_1$, such that $(T^*)^{-1}(\mathcal{U})$ is of wavelet-type, taking into account explicitly the ill-posedness due to T in (1). This is treated as a multiple testing problem of scanning type as in (2). As we will argue and illustrate in Section 1.2 for super-resolution microscopy, most important for designing such a multiscale test is to balance all local tests on the different scales in order to obtain good overall power taking into account the ill-posedness of the problem.

MISCAT works for non-identically distributed and non-Gaussian errors under a general moment condition including many practically relevant models. It is based on a proper scale calibration, which we employ for our test. The exact calibration depends on the dimension d , the denseness of scales in the dictionary, and the degree of average smoothness of the scanning functions, which implicitly takes into account the ill-posedness of the underlying problem (cf. Theorem 1 for general inverse problems and Theorem 2 for deconvolution). This is based on a general recipe for a proper choice of calibration (see Theorem 3), which is of independent interest. For example, this generalizes results by Sharpnack and Arias-Castro (2016) to other systems than rectangular scanning (see Remark 2), and to inverse problems and non-Gaussian errors. While the calibration proposed by Dümbgen and Spokoiny (2001) (which is frequently employed in multiscale procedures, see e.g. (Rohde, 2008; Walther, 2010)) applied to the dictionaries considered in this paper yields an overall test-statistic which converges to a degenerate limit (due to condition (SR) below), MISCAT is bounded from below and above by suitable Gumbel distributions, allowing to establish a non-degenerate limit of the test statistic.

A major benefit of MISCAT is its wide range of applicability. In addition to the potential use of

MISCAT for the aforementioned areas of application, in Sections 1.2 and 4.2. we discuss in more detail an example from protein imaging with super-resolution microscopy.

Fundamental to MISCAT are uniform confidence statements for the coefficients $\langle f, \varphi_i \rangle$, $1 \leq i \leq N$ in the inverse regression model (1). Conceptually related Söhl and Trabs (2012) and Nickl and Reiß (2012) provide uniform Donsker-type results in the context of deconvolution for single-scale contrasts $\langle f, \varphi \rangle$, however, not uniform in a multiscale dictionary \mathcal{U} .

In case that φ_i are chosen to have compact support, MISCAT allows to infer on the support of f . An important conclusion from our work is that the inverse problem causes a substantial difference to direct detection problems. As the operator T is typically smoothing, it is immediately clear that local properties of f are smoothed out in the sense that they may not be found as local properties of Tf anymore, as in general for f of bounded support the support of Tf is unbounded. This shows the crucial difference to the analysis carried out in (Holzmann et al., 2007; Laurent et al., 2011, 2012) where only global detection is considered. By inverting T explicitly by our method, we are, in fact, able to detect local properties of f in a multiscale fashion.

1.1 MISCAT

Let $\mathcal{U} = \{\varphi_i \mid 1 \leq i \leq N\} \subset \mathbb{H}_1$. We emphasize that, although in the formulation of the model (1) and the dictionary \mathcal{U} for ease of notation a dependence of the sample size n is not explicitly stated, all quantities may depend on n , i. e. $\mathcal{U} = \mathcal{U}(n)$, where the size of the dictionary $N = N(n)$ and the entries $\varphi_i = \varphi_i(n)$ may vary with n . In particular, we consider the case $N(n) \rightarrow \infty$ as $n \rightarrow \infty$. Our aim is to infer on $\langle f, \varphi_i \rangle$ simultaneously over $i \in \{1, \dots, N\}$. If $\varphi_i \in \mathcal{R}(T^*)$ for all $i \in \{1, \dots, N\}$, there exists a dictionary $\mathcal{W} = \{\Phi_i \mid 1 \leq i \leq N\} \subset \mathbb{H}_2$ such that $\varphi_i = T^*\Phi_i$. Then, using

$$\langle f, \varphi_i \rangle_{\mathbb{H}_1} = \langle Tf, \Phi_i \rangle_{\mathbb{H}_2}, \quad (3)$$

we may infer on $\langle f, \varphi_i \rangle$ via its empirical counterpart

$$\langle Y, \Phi_i \rangle_n := \frac{1}{n^d} \sum_{\mathbf{j} \in I_n} Y_{\mathbf{j}} \Phi_i(\mathbf{x}_{\mathbf{j}}). \quad (4)$$

We consider dictionaries \mathcal{W} of the following, wavelet-type structure

$$\mathcal{W} = \left\{ \Phi_i(\mathbf{z}) = \Phi \left(\frac{t_{i,1} - z_1}{h_{i,1}}, \dots, \frac{t_{i,d} - z_d}{h_{i,d}} \right) \mid \text{supp}(\Phi) \subset [0, 1]^d, i \in \{1, \dots, N\} \right\}, \quad (5)$$

and for $i \in \{1, \dots, N\}$, the vectors $\mathbf{h}_i = (h_{i,1}, \dots, h_{i,d})^T$ and the products $h_{i,1} \dots h_{i,d}$ are referred to as *scales* and *sizes of scales*, respectively.

The null-hypothesis of our testing problem is given by

$$H_0 : \langle f, \varphi_i \rangle = 0 \quad \forall \quad i \in \{1, \dots, N\}. \quad (6)$$

To account for multiplicity in (6), we aim at controlling the maximal value of the standardized version of the empirical coefficients, $\langle Y, \Phi_i \rangle_n$ as in (2), and study the asymptotic properties of a suitable Gaussian approximation. This approximation requires a coupling technique to replace the observation errors by i.i.d. Gaussian random variables. To this end we do not make use of strong approximations by KMT-like constructions (see (Komlós et al., 1975) for the classical KMT results and, e. g. (Rio, 1993) or (Dedecker et al., 2014) for generalizations) as, for instance, (Schmidt-Hieber et al., 2013) in the univariate case, $d = 1$. Doing so, they obtain the lower bound $\log(n)^3/n$ for the scale-size, and attempting to generalize this to $d > 1$ it can readily be seen from (Rio, 1993) that this lower bound is independent of d . Note that this is by far too restrictive, as it requires e.g. for a d -cube the side-length to be at least of order $n^{-1/d}$, up to a logarithmic factor. Therefore, we take a different route for $d \geq 2$ and employ a coupling of the supremum based on recent results by Chernozhukov et al. (2014). We will show that this allows for minimal

side-lengths of $n^{-1} \log(n)^{\frac{15}{d} \vee 3} \log \log(n)^2$ corresponding to $n^{-d} \log(n)^{15 \vee 3d} \log \log(n)^{2d}$ as lower bound on the sizes of the scales. There, the dimension enters in the right order, as it coincides with the sampling error (up to log factors).

MISCAT comprises a general class of scan statistics $\mathcal{S}(Y)$ as in (2) which are of the form,

$$\mathcal{S}(Y) := \max_{i \in \{1, \dots, N\}} S(Y, i), \quad \text{with} \quad S(Y, i) := \omega_i \left(\frac{|\langle Y, \Phi_i \rangle_n|}{\sigma_i} - \omega_i \right), \quad (7)$$

where $\sigma_i^2 := \text{Var}[\langle Y, \Phi_i \rangle_n]$ and

$$\omega_i = \sqrt{2 \log(C_{\Phi_i} / (h_{i,1} h_{i,2}))} + C_d \frac{\log(\sqrt{2 \log(C_{\Phi_i} / (h_{i,1} h_{i,2}))})}{\sqrt{2 \log(C_{\Phi_i} / (h_{i,1} h_{i,2}))}}$$

is a scale calibration (see Section 2). Here C_d is an explicit constant only depending on the dimension, the number of scales considered and the degree of L^2 -smoothness of Φ . The constants C_{Φ_i} can be numerically computed and depend on the local functions Φ_i (see (5) for the definitions of Φ and Φ_i). Theorem 1 in Section 2 provides a distribution free Gaussian approximation for the scan statistic (7) by replacing the errors by a standard Brownian sheet $W_{\mathbf{z}}$, i. e.

$$\mathcal{S}(W) := \max_{i \in \{1, \dots, N\}} S(W, i), \quad \text{with} \quad S(W, i) := \omega_i \left(\frac{|\int \Phi_i(\mathbf{z}) dW_{\mathbf{z}}|}{\|\Phi_i\|} - \omega_i \right). \quad (8)$$

Since $\mathcal{S}(W)$ does not depend on any unknown quantities, it can be used to simulate quantiles. For a wide-range of dictionary functions Φ , Theorem 1 guarantees that $\mathcal{S}(W)$ has a non-degenerate limit and the approximating quantiles are uniformly bounded as $n \rightarrow \infty$. In particular, it ensures the consistency of our multiscale-test with one-sided or two-sided alternative hypotheses

$$\exists i \in \{1, \dots, N\} : \quad H_1 : \langle f, \varphi_i \rangle > 0, \quad H_2 : \langle f, \varphi_i \rangle < 0 \quad \text{and} \quad H_3 : |\langle f, \varphi_i \rangle| > 0, \quad (9)$$

respectively. The multiscale test MISCAT for H_0 versus H_1 (see (6), (9)) with nominal level $1 - \alpha$ then works as follows. For each i , $\langle Y, \Phi_i \rangle_n$ is compared to the scale-dependent critical value $\hat{q}_{i,1-\alpha} := (\hat{q}_{1-\alpha} / \omega_i + \omega_i) \hat{\sigma}_i$, where $\hat{\sigma}_i^2$ is an estimate for σ_i^2 (cf. Remark 3) and $\hat{q}_{1-\alpha}$ is the (simulated) $1 - \alpha$ -quantile of $\mathcal{S}(W)$. If, for some i_0 , $\langle Y, \Phi_{i_0} \rangle_n > \hat{q}_{i_0,1-\alpha}$, the global null-hypothesis is rejected and, more specifically, our multiplicity adjustment allows us to identify those Φ_i as active components for which the empirical coefficients $\langle Y, \Phi_i \rangle_n$ are larger than $\hat{q}_{i,1-\alpha}$ at a controlled family-wise error rate.

1.2 Locating fluorescent markers in STED super-resolution microscopy

In Section 3, we specify and refine our results to deconvolution which is applied to a data example from nanobiophotonics in Section 4. Suppose that the operator T is a convolution operator acting on two-dimensional functions having a kernel k such that

$$(Tf)(\mathbf{y}) = \int_{\mathbb{R}^2} k(\mathbf{x} - \mathbf{y}) f(\mathbf{y}) d\mathbf{y}. \quad (10)$$

In our application (see Section 4.2) the convolution kernel k corresponds to the point spread function of a microscope and the object of interest, f , is an image such that $d = 2$. We assume that k is finitely smooth, which is equivalent to a polynomial decay of its Fourier coefficients. In this situation, we may choose the dictionaries \mathcal{U} and \mathcal{W} such that each $\varphi_i \geq 0$ has compact support $\text{supp}(\varphi_i) \subset [\mathbf{t} - \mathbf{h}, \mathbf{t}]$. Consequently, if $f \geq 0$, we find

$$\langle f, \varphi_i \rangle > 0 \quad \Rightarrow \quad \exists \mathbf{x} \in [\mathbf{t} - \mathbf{h}, \mathbf{t}] \quad \text{s.t.} \quad f(\mathbf{x}) > 0, \quad (11)$$

i. e. there must be a point $\mathbf{x} \in [\mathbf{t} - \mathbf{h}, \mathbf{t}]$ belonging to the support of f . Employing this, we can use MISCAT to segment f into active and (most likely) inactive parts, which is of particular interest

in many imaging modalities. To obtain (asymptotically) optimal detection properties of the test, we also discuss an optimal choice of probe functions φ_i in Section 4.

In Section 4.2 we infer on the location of fluorescent markers in DNA origami imaged by a super-resolution STED microscope, cf. (Hell, 2007). In STED microscopy, the specimen is illuminated by a laser beam along a grid with a diffraction-limited spot centered at the current grid point and the entire specimen is scanned this way, pixel by pixel. To enhance spatial resolution, the specimen is at the same time irradiated with a ring-like beam for inhibition. This reduces the size of the region from which light is collected, leading to observations of the form (1) with a convolution T as in (10). The error distribution and the kernel k in (10) are well-known experimentally, see Section 4.2 for details. The investigated specimen consists of DNA origami, which have been designed in a way such that each of the clusters contains up to 24 fluorescent markers, arrayed in two strands of up to 12 having a distance of 71 nanometers (nm) (cf. the sketch in the upper left of Figure 1). As the ground truth is basically known, this serves as a real world phantom. Data were provided by the lab of Stefan Hell of the Department of NanoBiophotonics of the Max Planck Institute for Biophysical Chemistry, cf. Figure 1.

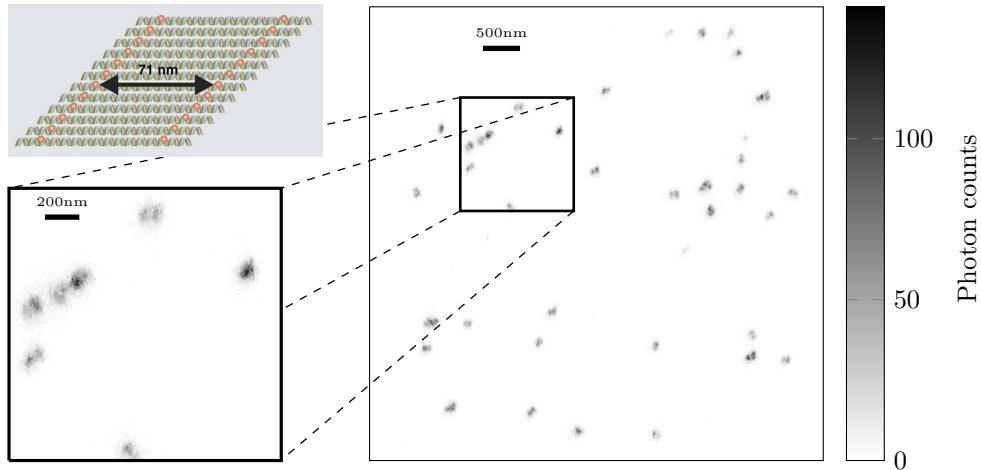


Figure 1: Experimental data of the DNA origami sample and zoomed region (150×150 pixels). The sketch in the upper left shows the structure of the investigated DNA origami sample (red dots represent possible positions for fluorophores) see (Ta et al., 2015)).

To infer on the positions of the fluorescent markers, we applied MISCAT with a set of scales defined by boxes of size $k_x \times k_y$ pixels, $k_x, k_y = 4, 6, \dots, 20$. One pixel in the measurements in Figure 1 is of size $10 \text{ nm} \times 10 \text{ nm}$. To highlight our multiscale approach we also applied a single scale test using only boxes of size 4×6 pixels (these are the smallest boxes found by MISCAT), and to highlight the deconvolution effect, we applied a direct multiscale scanning test not designed for deconvolution (i.e. $T = \text{id}$ in the model (1) and $\Phi_i = \varphi_i$ in (7)) based on indicator functions as probe functionals using the scale calibration suggested by Dümbgen and Spokoiny (2001).

In Figure 2 the zoomed region of Figure 1 is shown together with *significance maps* for all three tests. The significance map color-codes for each pixel the smallest scale on which it is significant. For example, in Figure 2(d) MISCAT marked several boxes as significant, and the smallest scale on which significant boxes were found is of size 2400 nm^2 . Any pixel contained in such a box is marked in yellow, and in Figure 2(d) four of these boxes were found. The other colors indicate pixels which belong to larger boxes marked as significant. In case that a pixel belongs to significant boxes of different scales, only the smallest one is displayed for ease of visualization by the color coding.

From the results in Figure 2(d) it is apparent that MISCAT is able (at least for some of the single DNA origamis) to distinguish both strands. In view of the zoomed data in Figure 2(b) and Figure 2(c) this is quite remarkable as not visible from the data. The single scale variant

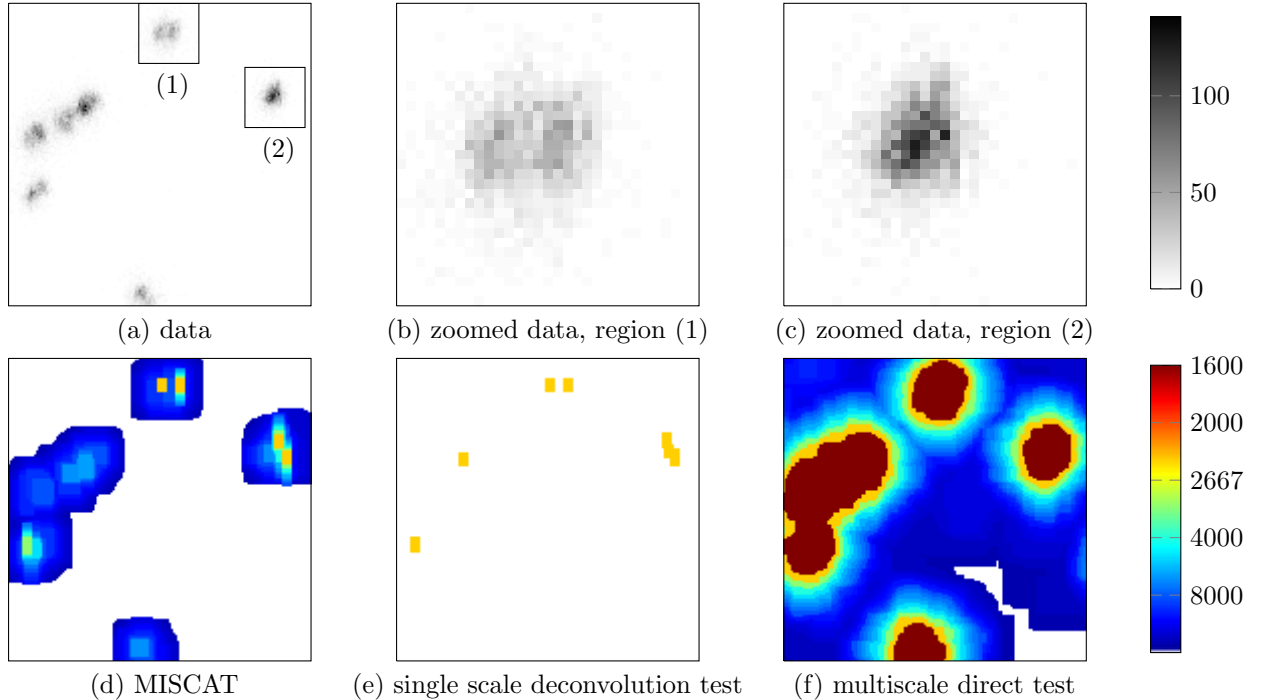


Figure 2: Experimental data and corresponding 90% significance maps computed by different tests. The color-coding of the significance maps always show the size of smallest significance in nm^2 , cf. the main text. (a)–(c) data and zoomed regions, (d) MISCAT, (e) a single scale test with deconvolution, (f) a multiscale scanning test without deconvolution.

of MISCAT (for explanation see below) in Figure 2(e) has clearly more power in detecting small features (i.e. there are more active boxes of size 4×6 pixels), but at the price of overseeing many DNA origamis. It is also clearly visible in Figure 2(f) that ignoring the deconvolution does not lead to a competitive test: distinguishing between different DNA origamis fails completely, as the support of the DNA-origami has been severely blurred by the STED microscope.

Note that the investigated specimen consists only of structures, which are present on a few (known) scales. For illustrative purposes, MISCAT, as employed here, does not use this information, as in general, these scales are not a priori known in living cell imaging. However, we stress that our method can be adapted immediately to the situation when a priori scale information is available by considering not all scales in a certain range but only a (small) subset. This will further increase detection power. To this end, the scale calibration has to be adjusted according to the complexity of the set of scales to preserve non-degenerateness of the limiting distribution as we will show in Section 5, Corollary 1 (see also Remark 2.2).

2 General Theory

2.1 Framework and Notation

Recall the general framework introduced in Section 1 and assume that we have access to data following model (1) and that the dictionary may depend on the sample size n . Furthermore, in model (1), n stands for the level of discretization such that, more rigorously, the model reads $Y_{\mathbf{j},n} = Tf(\mathbf{x}_{\mathbf{j},n}) + \xi_{\mathbf{j},n}$. For ease of notation, this dependence is dropped whenever it is not relevant. Throughout this paper, $\{Tf(\mathbf{x}_{\mathbf{j},n}) \mid \mathbf{j} \in I_n\}$ is the discretization of the function Tf on the grid $\{(j_1/n, \dots, j_d/n) \mid 1 \leq j_k \leq n, 1 \leq k \leq d\}$. This discretization model is a prototype for many inverse problems and in particular matches the application to imaging considered in Section 4

below. For different applications alternative discretization schemes may be of interest as well but, for the sake of a clearer display, we consider uniform sampling on a complete grid since most of the results presented below do not crucially depend on the specific discretization. We make the following assumption on the dictionary.

Assumption 1.

Let

a) (Dictionary source condition)

$$\varphi_i \in \mathcal{R}(T^*) \quad \text{such that} \quad \varphi_i = T^* \Phi_i. \quad (\text{DSC})$$

b) (Growth of the dictionary) For some $\kappa > 0$

$$|\mathcal{U}| = |\mathcal{W}| = N = O(n^\kappa). \quad (\text{G})$$

c) (Scale restrictions) For $\mathbf{h}_{\min} = (h_{\min}, \dots, h_{\min})^T$ and $\mathbf{h}_{\max} = (h_{\max}, \dots, h_{\max})^T$ the smallest and the largest scale considered, respectively,

$$h_{\min} \gtrsim n^{-1} \log(n)^{15/d \vee 3} \log \log(n)^2 \quad \text{and} \quad h_{\max} = o(\log(n)^{-2}). \quad (\text{SR})$$

d) (Average Hölder condition) Suppose that Φ in (5) is uniformly bounded, supported on $[0, 1]^d$, vanishing at the boundary and

$$\int |\Phi(\mathbf{t} - \mathbf{z}) - \Phi(\mathbf{s} - \mathbf{z})|^2 d\mathbf{z} \leq L_\Phi \|\mathbf{t} - \mathbf{s}\|_{l^2}^{2\gamma}, \quad (\text{AHC})$$

for some $\gamma \in [1/2, 1]$.

Remark 1.

1. Assumption (DSC) is a smoothness condition on the functions of the dictionary \mathcal{U} related to T . The most common assumption is the so-called benchmark source condition $f \in \mathcal{R}(T^*)$, which requires the unknown solution f to be at least as smooth as any function in the range of T^* . For deconvolution problems with real-valued kernel this means that f is at least as smooth as the kernel itself. In this paper, as we want to reconstruct pairings $\langle f, \varphi_i \rangle$ instead of f , we may pose conditions on the functions φ_i instead of f , see also (Burger et al., 2013). Note, that if additionally f admits a sparse representation w.r.t. the dictionary \mathcal{U} , then (DSC) implies $f \in \mathcal{R}(T^*)$. We emphasize that our approach strongly relies on the condition (DSC). However, from Lemma 1 in (Donoho, 1995), it follows that it is inevitable to pose such a condition, and exploiting (DSC) to reconstruct pairings $\langle f, \varphi_i \rangle$ is a well-known approach in inverse problems (Anderssen, 1986; Mathé and Pereverzev, 2002).
2. Assumption (G) is rather mild. In particular it implies that positions and scales $(\mathbf{t}_i, \mathbf{h}_i)$ from any grid of polynomial size can be used. In the example of imaging this is naturally satisfied as the \mathbf{t}_i are grid points of the pixel grid and the sizes of the scales \mathbf{h}_i are given by rectangular groups of pixels and are hence also only of polynomial order in n . Furthermore, to serve as an approximation for a continuous version, the grid can be chosen sufficiently fine and still (G) is satisfied. The constant κ only enters into our results via some constants.
3. As already discussed in the introduction, the scale restrictions (SR) are also rather mild. The lower bound on h_{\min} is up to a poly-log factor of the same order as the sampling error, and the upper bound on h_{\max} is required to ensure unbiasedness of our local test statistics. For some of the results presented below, a slightly stricter bound on h_{\max} will be necessary, and this is emphasized in the corresponding theorems.
4. Assumption (AHC) is a smoothness conditions on the dictionary \mathcal{W} . It is satisfied, for instance, if Φ is Hölder-continuous of order γ . $\Phi = I_{[0,1]^d}$ satisfies condition (AHC) with $\gamma = 1/2$ and $L_\Phi = d$.

The following assumptions concern the noise $\xi_{\mathbf{j}}$, $\mathbf{j} \in I_n$ in model (1).

Assumption 2. Let $\xi_{\mathbf{j}}$, $\mathbf{j} \in I_n$ in (1) be independent and centered random variables. Assume that there exists a function $\sigma \in C^1[0, 1]^d$ such that $\text{Var}[\xi_{\mathbf{j}}] = \sigma^2(\mathbf{x}_{\mathbf{j}})$ and

$$\mathbb{E}|\xi_{\mathbf{j}}|^{2J} \leq \frac{1}{2} J! \mathbb{E}\xi_{\mathbf{j}}^4 \quad \forall J \geq 2. \quad (\text{M1})$$

Assume further that

$$0 < \liminf_{n \rightarrow \infty} \inf_{\mathbf{j} \in I_n} \mathbb{E}[|\xi_{\mathbf{j}}|^2] \quad \text{and} \quad \limsup_{n \rightarrow \infty} \sup_{\mathbf{j} \in I_n} \mathbb{E}[|\xi_{\mathbf{j}}|^4] < \infty. \quad (\text{M2})$$

2.2 Asymptotic Theory

Given the simple form of $\langle Y, \Phi_i \rangle_n$ in (4), one might be inclined to use the quantiles from the maximum of a Gaussian version for the construction of the confidence statements on $\langle f, \varphi_i \rangle$ as long as both quantities are asymptotically close to each other. This approach is, however, problematic. While the fact that the maximum statistic is in general unbounded as n tends to infinity is captured by the rate of growth of the quantiles, the fact that, in a multiscale setting, some elements of the dictionary completely dominate the behavior of the maximum of the statistic should be corrected in a suitable way as it was already pointed out by Dümbgen and Spokoiny (2001), followed by other authors. To this end, a scale calibration should be included that ensures that the contributions for all indices in the maximum are comparable.

In this paper, we consider wavelet-type dictionaries defined in (5), where, with a slight abuse of notation, we abbreviate

$$\Phi\left(\frac{t_{i,1} - z_1}{h_{i,1}}, \dots, \frac{t_{i,d} - z_d}{h_{i,d}}\right) = \Phi\left(\frac{\mathbf{t}_i - \mathbf{z}}{\mathbf{h}_i}\right).$$

Here, $(\mathbf{t}_i, \mathbf{h}_i) \in \{(\mathbf{t}_i, \mathbf{h}_i) \mid i = 1, \dots, N, \mathbf{h}_i \in (0, 1]^d, \mathbf{t}_i \in [\mathbf{h}_i, \mathbf{1}]\}$. Recall that, typically, $N = N(n)$ and, as $n \rightarrow \infty$, also $N(n) \rightarrow \infty$ and $h_{i,l} \rightarrow 0, l = 1, \dots, d$.

Theorem 1.

Given observations from model (1) with random noise satisfying Assumption 2, dictionaries \mathcal{U} and \mathcal{W} as specified in Assumption 1 such that, in addition, \mathcal{W} satisfies the wavelet assumption (5). Let $h_{\max} \leq n^{-\delta}$ for some (small) $\delta > 0$ and suppose that the approximation error of $\langle \mathbb{E}[Y], \Phi_i \rangle_n := \frac{1}{n^d} \sum_{\mathbf{j} \in I_n} T f(\mathbf{x}_{\mathbf{j}}) \Phi_i(\mathbf{x}_{\mathbf{j}})$ is asymptotically negligible, i. e.,

$$\max_{1 \leq i \leq N} n^{\frac{d}{2}} \frac{\langle \mathbb{E}[Y], \Phi_i \rangle_n - \langle T f, \Phi_i \rangle}{\|\Phi_i\|_2} = o\left(\frac{1}{\log(n)^2 \log \log(n)^2}\right). \quad (12)$$

For any constant $K \geq 1$, define $\lambda_i(K) := \sqrt{2 \log(K / (h_{i,1} \dots h_{i,d}))}$, $C_d = 2d + d/\gamma - 1$ and

$$\omega_i(K, C_d) = \omega_i := \lambda_i(K) + C_d \frac{\log(\lambda_i(K))}{\lambda_i(K)}. \quad (13)$$

Then, for a standard Brownian sheet $W_{\mathbf{z}}$, it holds

$$\lim_{n \rightarrow \infty} \left| \mathbb{P}_{H_0}(\mathcal{S}(Y) > q) - \mathbb{P}_{H_0}(\mathcal{S}(W) > q) \right| = 0, \quad q \in \mathbb{R}$$

where $\mathcal{S}(Y)$ and $\mathcal{S}(W)$ are defined in (7) and (8), respectively. The approximating statistic $\mathcal{S}(W)$ is almost surely bounded and does not depend on the unknown quantities.

Moreover, if for some constants $1/2 < \gamma \leq 1$, $L_{\Phi} > 0$

$$\int |\Phi(\mathbf{t} - \mathbf{z}) - \Phi(\mathbf{s} - \mathbf{z})|^2 d\mathbf{z} = L_{\Phi} \sum_{j=1}^d |t_j - s_j|^{2\gamma} + o\left(\sum_{j=1}^d |t_j - s_j|^{2\gamma}\right), \quad (\text{AHCb})$$

and the grids of positions \mathbf{t} and scales \mathbf{h} are sufficiently fine, i.e.

$$\max_{1 \leq i \leq N} \min_{1 \leq j \leq N: \mathbf{t}_i \neq \mathbf{t}_j} \|\mathbf{t}_i - \mathbf{t}_j\|_\infty = O\left(\frac{1}{n}\right) \quad (14)$$

and

$$\min_{1 \leq j \leq N} \left| \frac{1}{h_{i,l}} - \frac{1}{h_{j,l}} \right| = o\left(\frac{1}{h_{i,l}} \wedge \frac{1}{h_{j,l}}\right), \quad (15)$$

then $\mathcal{S}(W)$ is bounded from below in probability and is asymptotically non-degenerate.

All proofs will be given in Section 6.

Remark 2.

1. Note that assumption (12) is only a mild assumption on the integral approximation as the required rate is very slow. It is satisfied, in particular, if Tf and Φ in (5) are Hölder-continuous of some order, or if Tf is Hölder-continuous and Φ is an indicator function. Note that due to the ill-posedness of the problem, Tf being Hölder-continuous does typically not require f to be continuous.
2. Although it might seem marginal, a proper choice of the constant C_d is crucial for the boundedness of $\mathcal{S}(W)$. The choice $C_d = 2d + d/\gamma - 1$ used in the formulation of the theorem is adjusted to the case where a dense grid of scales in the sense of (15) is considered. In particular, this includes the case where **all** scales in Assumption 1 (SR) ranging from \mathbf{h}_{\min} to \mathbf{h}_{\max} are used. If now, for instance, $T = \text{id}$ and Φ in (5) is chosen to be the indicator function of $[0, 1]^d$, we have $\gamma = 1/2$ and consequently $C_d = 4d - 1$, which agrees with the constant in the weak convergence result of Sharpnack and Arias-Castro (2016) for the Gaussian case.

However, in many situations a less dense grid of scales might be of interest, e.g. under prior scale information on the object of interest f . For the choice $C_d = 2d + d/\gamma - 1$ the statistic $\mathcal{S}(W)$ is still a.s. bounded from above, but the boundedness from below might get lost. To avoid this, C_d has to be adjusted. Suppose in what follows that the grid of positions still satisfies (14). In the least dense regime, when $\mathcal{S}(W)$ behaves as in a single scale scenario, the proper choice is $C_d = d/\gamma - 1$. Another interesting special case is when only squares in a dense range are considered (this is $\mathbf{h}_i = (h_i, \dots, h_i)$ and (15) is satisfied), one should choose $C_d = 1 + d/\gamma$.

All these choices of C_d are specified in more detail in Corollary 1 in Section 5.

3. As specified in the theorem, $\mathcal{S}(W)$ is bounded for any choice of the constant $K \geq 1$. In fact, K only determines the location of the limiting distribution. However, there are 'natural' choices for K in the special cases $\gamma = 1/2$ and $\gamma = 1$ from extreme value theory. They are given in Theorem 3 in Section 5.

2.3 Statistical Inference

Theorem 1 guarantees in particular that the quantiles of $\mathcal{S}(Y)$ can be approximated by the quantiles of $\mathcal{S}(W)$. Let $q_{1-\alpha}^{\mathcal{S}(W)}$ denote the $1 - \alpha$ -quantile of the approximating process $\mathcal{S}(W)$. Define the scale dependent quantiles

$$q_{i,1-\alpha} := \left(\frac{q_{1-\alpha}^{\mathcal{S}(W)}}{\omega_i} + \omega_i \right) \sigma_i, \quad (16)$$

where $\sigma_i^2 = \text{Var}[\langle Y, \Phi_i \rangle_n]$.

Remark 3. Note that the local variances σ_i^2 , $1 \leq i \leq N$, depend on $\text{Var}[\xi_{\mathbf{j}}] = \sigma^2(\mathbf{x}_{\mathbf{j}})$ (cf. Assumption 2), $\mathbf{j} \in I_n$, which are typically unknown in applications. Nevertheless, all results remain valid if the C^1 -function σ^2 can be estimated from the data by $\hat{\sigma}^2$ such that

$$\max_{1 \leq i \leq N} |\hat{\sigma}^2(\mathbf{t}_i) - \sigma^2(\mathbf{t}_i)| = o_{\mathbb{P}} \left(\frac{1}{\sqrt{\log(n)}} \right). \quad (\text{V})$$

The local variances σ_i^2 can then be estimated by $\hat{\sigma}_i^2 := \langle \hat{\sigma}^2, \Phi_i^2 \rangle_n$. Condition (V) is e.g. satisfied for (suitable) kernel-type estimators or point-wise maximum likelihood estimators as used in Section 4.2.

Using (16), we conclude by Theorem 1 that

$$\lim_{n \rightarrow \infty} \mathbb{P}_{H_0} (|\langle Y, \Phi_i \rangle_n| \leq q_{i,1-\alpha} \quad \forall i \in \{1, \dots, N\}) \geq 1 - \alpha.$$

Hence, with overall confidence of approximately $(1 - \alpha) \cdot 100\%$ all probe functions φ_i such that $\langle Y, \Phi_i \rangle_n > q_{i,1-\alpha}$ are significant. Conversely, the following lemma guarantees that, with overall confidence of approximately $(1 - \alpha) \cdot 100\%$, all relevant components are found, provided that the signal is sufficiently strong.

Lemma 1. Given observations from model (1) with random noise satisfying Assumption 2, dictionaries \mathcal{U} and \mathcal{W} as specified in Assumption 1 such that, in addition, \mathcal{W} satisfies the wavelet assumption (5). For $k \in \{1, 2\}$, let $\mathcal{I}_{k,\alpha}$ denote the set of all large components, i. e.

$$\mathcal{I}_{k,\alpha} := \{i \mid (-1)^k \langle \varphi_i, f \rangle > 2q_{i,1-\alpha}\}.$$

Then, under the assumptions of Theorem 1

$$\lim_{n \rightarrow \infty} \mathbb{P} \left((-1)^k \langle Y, \Phi_i \rangle_n > q_{i,1-\alpha} \quad \forall i \in \mathcal{I}_{k,\alpha}, k = 1, 2 \right) \geq 1 - \alpha$$

3 Deconvolution

In our data example, presented in Section 4 below, we are dealing with images from fluorescence microscopy. Therefore we will formulate the following results concerning deconvolution problems only for $d = 2$, generalization to arbitrary d is straight forward. In order to describe the data, we consider the following special case of the general inverse regression model (1):

$$Y_{\mathbf{j}} = (k * f)(\mathbf{x}_{\mathbf{j}}) + \xi_{\mathbf{j}}, \quad \mathbf{j} \in \{1, \dots, n\}^2. \quad (17)$$

In model (17), the function k is a convolution kernel which corresponds to the point-spread function (PSF) of the microscope, see (Aspelmeier et al., 2015; Bertero et al., 2009), and the operation “ $*$ ” denotes convolution as defined in (10).

Assume that there exist positive constants \underline{c}, \bar{C} and a such that

$$\underline{c}(1 + \|\xi\|_2^2)^{-a} \leq |\mathcal{F}k(\xi)| \leq \bar{C}(1 + \|\xi\|_2^2)^{-a} \quad (\text{D1})$$

where \mathcal{F} denotes the Fourier transform. Assumption (D1) is a standard assumption characterizing mildly ill-posed deconvolution problems, see, e. g. (Meister, 2009).

3.1 Theory

The specific structure of T being a convolution with kernel k allows us to choose a dictionary \mathcal{U} such that $\varphi_i \geq 0$ and $\text{supp}(\varphi_i) \subset [0, 1]^d$ for all $1 \leq i \leq N$. Consequently we can infer directly on

the support of the signal f using the coefficients $\langle f, \varphi_i \rangle$ as discussed in (11). We can write for a dictionary as in (5)

$$\left\langle f, \varphi\left(\frac{\mathbf{t} - \cdot}{\mathbf{h}}\right) \right\rangle = \left\langle f * k, \tilde{\Phi}_{\mathbf{h}}\left(\frac{\mathbf{t} - \cdot}{\mathbf{h}}\right) \right\rangle,$$

where $\tilde{\Phi}_{\mathbf{h}}$ depends on \mathbf{h} as follows

$$\tilde{\Phi}_{\mathbf{h}} := \mathcal{F}^{-1}\left(\frac{\mathcal{F}\varphi}{\mathcal{F}k(\cdot/\mathbf{h})}\right). \quad (18)$$

In particular, the wavelet-type structure of the dictionary \mathcal{U} is transferred to the dictionary \mathcal{W} . Starting from the class

$$\mathcal{U} = \left\{ \varphi_i \mid \varphi_i(\mathbf{z}) = \varphi\left(\frac{\mathbf{t}_i - \mathbf{z}}{\mathbf{h}_i}\right), i \in \{1, \dots, N\} \right\},$$

generated by a single, sufficiently smooth, fixed function $\varphi \in \mathcal{R}(T^*) = \mathcal{R}(T)$, we obtain

$$\mathcal{W} = \left\{ \Phi_i \mid \Phi_i(\mathbf{z}) = \tilde{\Phi}_i\left(\frac{\mathbf{t}_i - \mathbf{z}}{\mathbf{h}_i}\right), i \in \{1, \dots, N\} \right\}. \quad (19)$$

With such a construction of the dictionaries, the ill-posedness of the problem is fully encoded within the dictionary \mathcal{W} .

In Section 4, the convolution kernel k is chosen from the family $\{k_{a,b} \mid a \in \mathbb{N}, b > 0\}$ defined in Fourier space via

$$(\mathcal{F}k_{a,b})(\boldsymbol{\xi}) = (1 + b^2 \|\boldsymbol{\xi}\|_2^2)^{-a}, \quad \boldsymbol{\xi} \in \mathbb{R}^2. \quad (20)$$

This is a 2-dimensional generalization of the one-dimensional case of the family of auto-convolutions of a scaled version of the density of the Laplace distribution with itself with radially symmetric PSF. In our simulations we choose $a = 2$ and $b = 0.0243$ (see Figure 3), motivated by our data example in Section 4.2. In both situations, the parameter b was chosen such that the full width at half maximum (FWHM) matches a given value (see Figure 3 for an explanation of the FWHM). The FWHM is a common standard measure for the spread of a convolution kernel in optics, see e. g. (Hell and Wichmann, 1994; Pawley, 2006), and there is a common understanding that objects which are closer to each other than a distance of approximately the FWHM cannot be identified as separate objects.

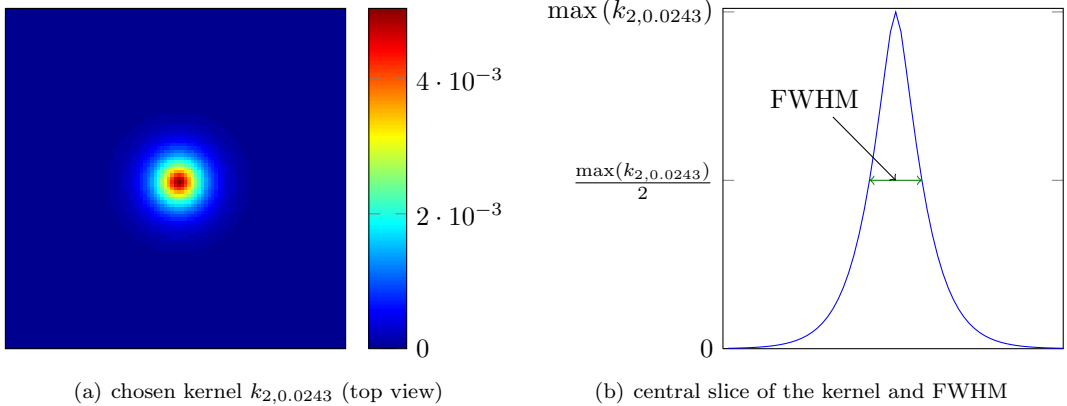


Figure 3: The function $k_{2,0.0243}$ and its full width at half maximum (FWHM).

For any convolution kernel $\psi_{a,b}$ Assumption (D1) is obviously satisfied and we obtain

$$\tilde{\Phi}_i = \sum_{j=0}^a \sum_{k=0}^j \binom{a}{j} \binom{j}{k} \left(\frac{b}{h_{i,1}}\right)^{2k} \left(\frac{b}{h_{i,2}}\right)^{2(j-k)} \partial^{(2k, 2(j-k))} \varphi. \quad (21)$$

This shows that a compactly supported function φ results in a dictionary \mathcal{W} which consists of compactly supported functions as well. Hence, the results from Theorem 3 carry over to deconvolution. Only assuming (D1), however, might result in a dictionary \mathcal{W} of functions of unbounded support. In this case the results from Theorem 1 remain valid if we exclude a small boundary region of the picture from our analysis. To this end we assume that we have available observations which are equidistantly sampled on the square $[-\rho, 1 + \rho]^2$ for some $\rho > 0$. While the complete dataset is used to estimate the coefficients, only the observations on $[0, 1]^2$ are used for the analysis, i. e., as before, only positions $\mathbf{t}_i \in [\mathbf{h}_i, \mathbf{1}]$ are considered. Then, uniformly in \mathbf{h} and \mathbf{t} , the empirical coefficients $\langle Y_{\mathbf{j}}, \Phi_{\mathbf{h}} \rangle_n \approx \int \Phi_{\mathbf{h}}(\mathbf{z}) \mathbb{1}_{[-\rho, 1 + \rho]^2}(\mathbf{z}) dW_{\mathbf{z}}$ can be approximated by $\int \Phi_{\mathbf{h}}(\mathbf{z}) dW_{\mathbf{z}}$ even if $\Phi_{\mathbf{h}}$ is of unbounded support. Hence, in the general deconvolution setting, we consider the model

$$Y_{\mathbf{j}} = (k * f)(\mathbf{x}_{\mathbf{j}}) + \xi_{\mathbf{j}}, \quad \mathbf{j} \in I_n^\rho := \{-\lfloor \rho n \rfloor, \dots, \lfloor n(1 + \rho) \rfloor\}^2, \quad \rho > 0, \quad (22)$$

where, as before, $\mathbf{x}_{\mathbf{j}} = \frac{1}{n} \cdot \mathbf{j}$.

Theorem 2.

Suppose that we have access to observations following model (22) with convolution kernel k satisfying Assumption (D1) and random noise satisfying Assumption 2. If the dictionary is given by (19) with dictionary function $\tilde{\Phi}_{\mathbf{h}}$ defined in (18) such that Assumption 1 is satisfied and, in addition, φ belongs to a Sobolev space $H^{2a+\alpha}(\mathbb{R})$ for some $\alpha > 0$, $\|(h_2 \wedge h_1)^{2a} \tilde{\Phi}_{\mathbf{h}}\|_2$ is uniformly bounded from below and above.

Assume further that the approximation error of $\langle \mathbb{E}[Y], \Phi_i \rangle_n := \frac{1}{n^d} \sum_{\mathbf{j} \in I_n} T f(\mathbf{x}_{\mathbf{j}}) \Phi_i(\mathbf{x}_{\mathbf{j}})$ is asymptotically negligible, i. e.,

$$\max_{1 \leq i \leq N} n^{\frac{d}{2}} \frac{\langle \mathbb{E}[Y], \Phi_i \rangle_n - \langle T f \mathbb{1}_{[-\rho, 1 + \rho]^2}, \Phi_i \rangle}{\|\Phi_i\|_2} = o\left(\frac{1}{\log(n)^2 \log \log(n)^2}\right). \quad (23)$$

The the results of Theorem 1 carry over to this general convolution setting under the same additional assumptions.

3.2 Signal Detection

In this section we specify the results from Section 2.3 for deconvolution.

Lemma 2. Given observations from model (1) with random noise satisfying Assumption 2 and k as in (20) and given $\varphi \in \mathcal{R}(T^*)$, define the dictionary \mathcal{W} as in (19) with dictionary function (18). For $k \in \{1, 2\}$, let $\mathcal{I}_{k,\alpha}$ denote the set

$$\mathcal{I}_{k,\alpha} := \{i \mid (-1)^k \langle \varphi_i, f \rangle > 2q_{i,1-\alpha} \|\sigma \Phi_{\mathbf{h}_i}\|_2 / n^{d/2}\}.$$

Then, under the assumptions of Theorem 1,

$$\lim_{n \rightarrow \infty} \mathbb{P}_{H_0}((-1)^k \langle \Phi_i, Y \rangle_n > q_{i,1-\alpha} \|\sigma \Phi_{\mathbf{h}_i}\|_2 / n \quad \forall i \in \mathcal{I}_{k,\alpha}, k = 1, 2) \geq 1 - \alpha.$$

Note, that $\|\Phi_{\mathbf{h}}\|_2 \sim \sqrt{h_1 h_2} (h_1 \wedge h_2)^{-2a}$. In particular, the previous lemma implies the consistency of the testing procedure, whenever $a = 1$ or $h_{\min} \gtrsim (\log(n)/n)^{1/(4a-1)}$.

Lemma 3. Given observations from model (1) with random noise satisfying Assumption 2 and k as in (20) and given a non-negative function $\varphi \in \mathcal{R}(T^*)$, define the dictionary \mathcal{W} as in (19)

with dictionary function (18). Suppose that the signal f is non-negative as well. Let further $\mathcal{I}_\alpha(f)$ denote the set

$$\mathcal{I}_\alpha(f) := \{i \mid f|_{\text{supp}(\varphi_i)} > 2q_{i,1-\alpha} \|\sigma\Phi_{\mathbf{h}_i}\|_2 / (h_{i,1} h_{i,2} n^{d/2})\}.$$

Then, under the assumptions of Theorem 1,

$$\lim_{n \rightarrow \infty} \mathbb{P}(\langle \Phi_i, Y \rangle >_n q_{i,1-\alpha} \|\sigma\Phi_{\mathbf{h}_i}\|_2 / n \quad \forall i \in \mathcal{I}_\alpha(f)) \geq 1 - \alpha.$$

The previous lemma implies the consistency of the testing procedure for the signal itself, i. e., testing $f = 0$ versus $f > 0$, if the minimal scale satisfies $h_{\min} \gtrsim (\log(n)/n)^{1/(4a+1)}$. In model (22) and under the Assumptions of Theorem 2, the previous Lemmas also hold for the deconvolution setting (D1).

For a comparison consider the rate of estimation of the $2a$ -th derivative of a Hölder β function w.r.t L^∞ risk in $d = 1$. We restrict to this case as otherwise the deconvolution is no longer equivalent to estimating derivatives, cf. (21). This is possible with rate

$$\left(\frac{\log n}{n}\right)^{\beta/(2\beta+4a+1)},$$

which is attained for $h \sim (\log n/n)^{1/(2\beta+4a+1)}$, see e.g. (Johnstone et al., 2004), i.e. such a function can be distinguished from 0 by means of estimation on a box $[t-h, t]$ as long as it is asymptotically larger than h^β . Posing the same question to MISCAT, the above result show that for $f|_{[t-h, t]} \sim h^\beta$ and $h \sim (\log n/n)^{1/(2\beta+4a+1)}$ it marks $[t-h, t]$ as active with (asymptotic) probability $\geq 1 - \alpha$. Consequently any support points found by estimation will also be found by MISCAT.

4 Simulations and real data applications

In this section we investigate the finite sample properties of the proposed multiscale test. To this end, we apply the test in a 2-dimensional mildly ill-posed deconvolution problem. In Section 4.2 we then analyze experimental STED data to locate single DNA origami in a sample.

Specifying the setting described in Section 3 to this situation, the data is given by (17).

The convolution kernel k is chosen from the two-parameter family $\{k_{a,b} \mid a \in \mathbb{N}, b > 0\}$ defined in Fourier space in (20).

4.1 2-dimensional support inference

Now we will infer on the support of a testfunction of realistic size from simulated data. In accordance with our data example we choose $n = 512$, and the kernel parameters are set to $a = 2$ and $b = 0.0243$. This implies that the decay order of the convolution kernel in Fourier space is 4 and the full width at half maximum (FWHM) of $k_{a,b}$ is about 10 pixels in the above setting (cf. Figure 3).

In this situation we investigate three tests, which differ in the choice of the probe function φ acting as mother wavelet. Obviously, the choice of φ has a high influence on the detection properties of the corresponding test via the variances $\|\sigma\tilde{\Phi}_{\mathbf{h}_i}\|_2^2$, which might e.g. be seen from Lemma 2. Extending an argument from (Schmidt-Hieber et al., 2013) for $d = 1$ to the general case, we can provide a mother wavelet φ which minimizes the asymptotic variance of the test statistic over all tensor-type probe functions. It only depends on the polynomial decay order of the convolution kernel in Fourier space ($\hat{=}$ degree of ill-posedness) and is given by

$$\varphi(x, y) = x^{\beta_1+1} (1-x)^{\beta_1+1} y^{\beta_2+1} (1-y)^{\beta_2+1} \mathbf{1}_{(0,1)}(x) \mathbf{1}_{(0,1)}(y), \quad (24)$$

where the two parameters $\beta_1, \beta_2 \in \mathbb{N}$ specify a priori knowledge of the ill-posedness in x and y direction, respectively. Ideally, the parameters β_1, β_2 should equal the polynomial decay order of the convolution kernel in x and y direction.

We now use three different setups:

Ψ_c **Correct setup.** In this case, the test uses the true ill-posedness, which corresponds to choosing $\beta_1 = \beta_2 = 2a = 4$.

Ψ_o **Oversmoothing setup.** In this case, the probe function is smoother than necessary, i.e. the ill-posedness is overspecified with $\beta_1 = \beta_2 = 10$. From a practitioners point of view, this choice can be considered to be pessimistic.

Ψ_u **Undersmoothing setup.** In this case, the probe function is not smooth enough, i.e. the ill-posedness is underestimated with $\beta_1 = \beta_2 = 1$. From a practitioners point of view, this choice can be considered to be optimistic.

In all of these cases, the constant C_Φ , appearing in the definition of the calibration ω_i in (13) is chosen by a numerical approximation of the formula (26) given in the appendix.

All our tests use 196 different scales defined by boxes consisting of $k_x \times k_y$ pixels, $k_x, k_y = 4, 6, \dots, 30$. Concerning the positions \mathbf{t} we again use all possible upper left points of boxes fitting in the image.

4.1.1 Boundedness of the approximating Gaussian version

Figure 4 shows histograms of 10.000 runs of the approximating Gaussian test statistic $\mathcal{S}(W)$. Note again that this statistic is independent of all unknown quantities including the variance due to the standardization of the local test statistics. The simulations suggest a stable behavior of the distribution of the maximum statistic for all three tests.

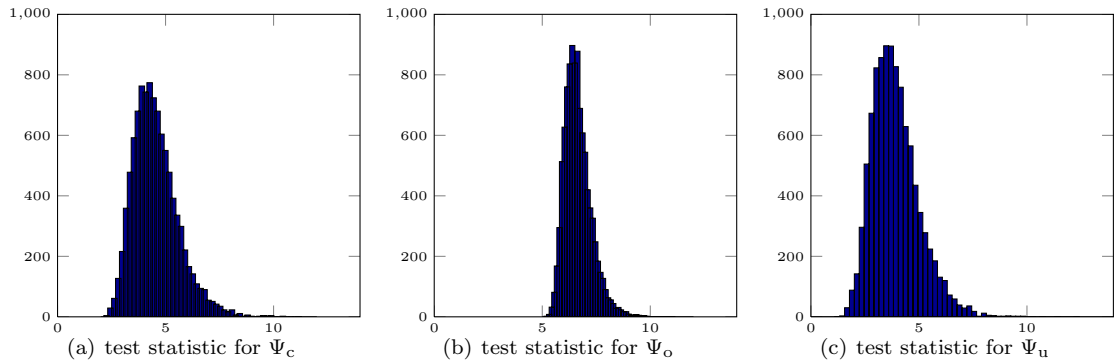


Figure 4: Histograms for 10^4 runs of the test statistic applied to pure Gaussian white noise.

4.1.2 Detection properties

To investigate more detailed the influence of the proper specification of ill-posedness via the three tests Ψ_c , Ψ_o and Ψ_u , empirical quantiles q_α are computed from the simulations in Figure 4, which are also shown in Table 1.

We expect the test to reach a twofold aim: To detect weak signals and to distinguish between different signals, strong enough (see Lemma 2). To illustrate the difference in power of the three tests, we show an exemplary simulation based on a synthetic testfunction which is a step-function with values in $\{0, 1\}$ (see Figure 5(a)). In agreement with our prospects, the testfunction consists of some comparably large and well-distributed circles (3 in the top row, 6 in the second row, 12

	α	0.1	0.5	0.8	0.9	0.95	0.99
Ψ_c	q_α	3.3420	4.4006	5.3194	5.8828	6.4722	7.6442
Ψ_o	q_α	5.9541	6.5553	7.1012	7.4512	7.7888	8.5752
Ψ_u	q_α	2.6635	3.7673	4.7307	5.3649	5.9227	7.1658

Table 1: Empirical quantiles of the test statistic for the three different test in Figure 4.

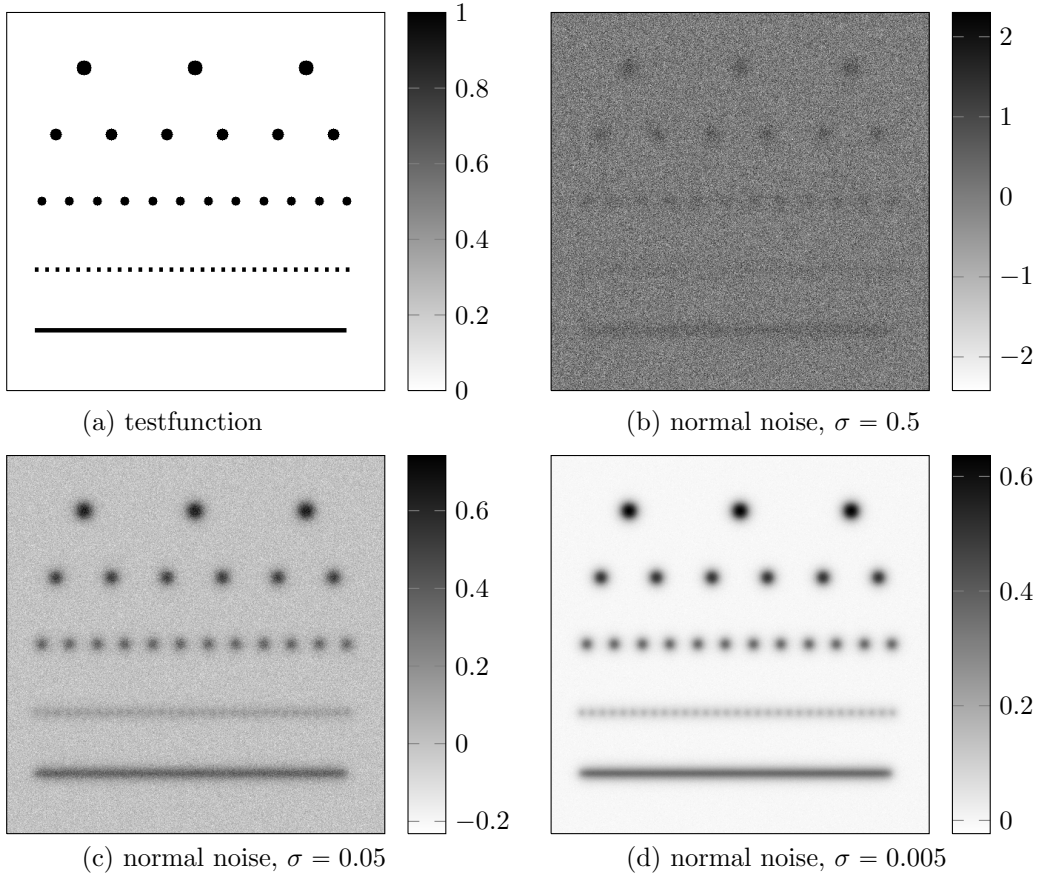


Figure 5: Synthetic testfunction and simulated data for three different noise levels $\sigma \in \{0.005, 0.05, 0.5\}$.

in the third row), of a line of squares in the fourth row, and of a continuous line of same height in the bottom row at different sizes.

For three different noise levels $\sigma \in \{0.005, 0.05, 0.5\}$ we simulate from a homogeneous Gaussian model (see Figure 5(b)–(d)). To avoid masking effects caused by variance estimation, we always use the true variance in our test statistic. In Figure 6 the data and the resulting significance maps for the three different tests are depicted. The significance map color-codes for each pixel the smallest scale on which it was significant. This means exemplary for the top left subfigure that the optimal test Ψ_c marked several boxes as significant, and the smallest scale on which significant boxes were found contains 624 pixels. Any pixel contained in such a box is marked in dark red, which is the case in the third object in the top row and in objects number 2 and 4 in the second row of the top left subfigure. The other colors indicate pixels which belong to larger boxes marked as significant. In case that a pixel belongs to significant boxes of different scales, the smallest one

is indicated by the color coding.

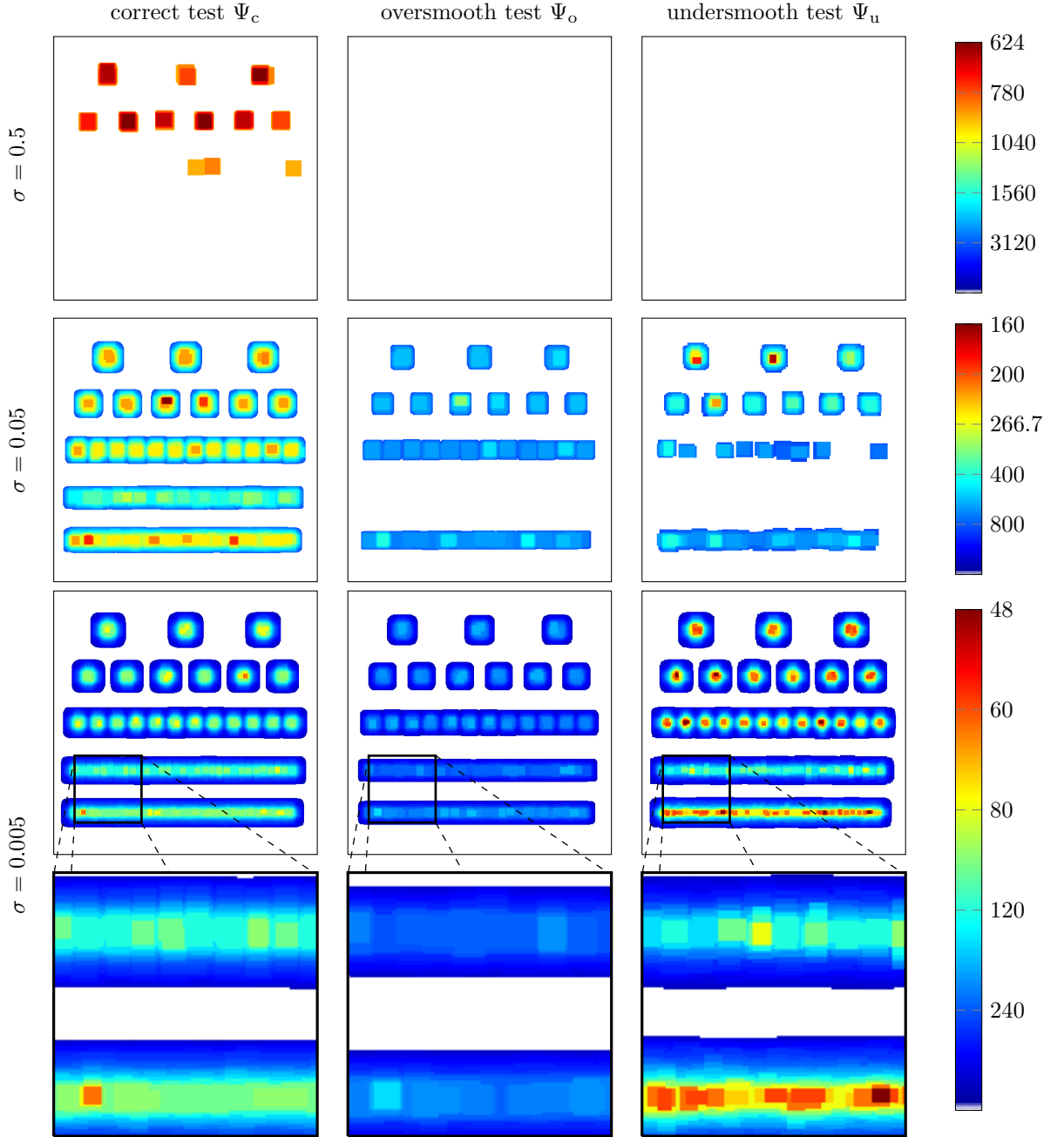


Figure 6: Support detected by the three different tests at 90%-significance level on the data from Figure 5. Each column corresponds to the results of a fixed test for different noise levels, each row to the results for the different tests for a fixed noise level. The color-coding shows the smallest scale (in pixels) on which the corresponding pixel was significant.

In conclusion we find that the optimal test Ψ_c measures up to our expectations. It detects the large objects even in the large noise regime Figure 5(b) (where the other two tests do not find any significant boxes), and from the zoomed plot in Figure 6, bottom left, it is apparent that Ψ_c is able to distinguish between the line in the bottom row and the sequence of squares in the second last row, i.e. it is able to distinguish objects which have a distance of 9 pixels, which is even less

than the FWHM.

It is immediately apparent that the undersmoothing test Ψ_u is more sensitive on small scales compared to Ψ_c and Ψ_o , but both Ψ_o and Ψ_u cannot keep up with the large scale detection power of Ψ_c , as this test is the only one to detect any signal in the large noise situation. From our theory (cf. Lemma 3) we know that a box B_i will be detected as soon as $f|_{B_i} \geq 2 \left(\frac{q_{1-\alpha}}{\omega_i} + \omega_i \right) \frac{\|\sigma \tilde{\Phi}_i\|_2}{\sqrt{h_{i,1} h_{i,2} n^d}}$ with probability $\geq 1 - \alpha$ (the penalties ω_i are as in Theorem 1 and $\tilde{\Phi}$ is the corresponding transformed mother wavelet as in Section 3.1). This provides the largest σ which still ensures a 90% detection,

$$\sigma = \frac{\sqrt{h_{i,1} h_{i,2} n^d}}{\|\tilde{\Phi}_i\|_2} \left(2 \left(\frac{q_{1-\alpha}}{\omega_i} + \omega_i \right) \right)^{-1}.$$

Numerical approximations of the values of the right-hand side are depicted in Figure 7 against the size (being $h_{i,1} h_{i,2}$) of the considered scales. For visual appeal, the computed values have been smoothed. Comparing Ψ_c and Ψ_u it becomes apparent that Ψ_u allows for more detections on small scales, but will necessarily oversee several weak signals on large scales. Comparing Ψ_c and Ψ_o we find that Ψ_o has less detection power on all considered scales. Concerning Ψ_o and Ψ_u it seems that Ψ_u has better detection properties on nearly all scales but the largest ones. In conclusion one might draw the advice to better underestimate the ill-posedness than to overestimate it, but nevertheless good knowledge of the ill-posedness is very helpful.

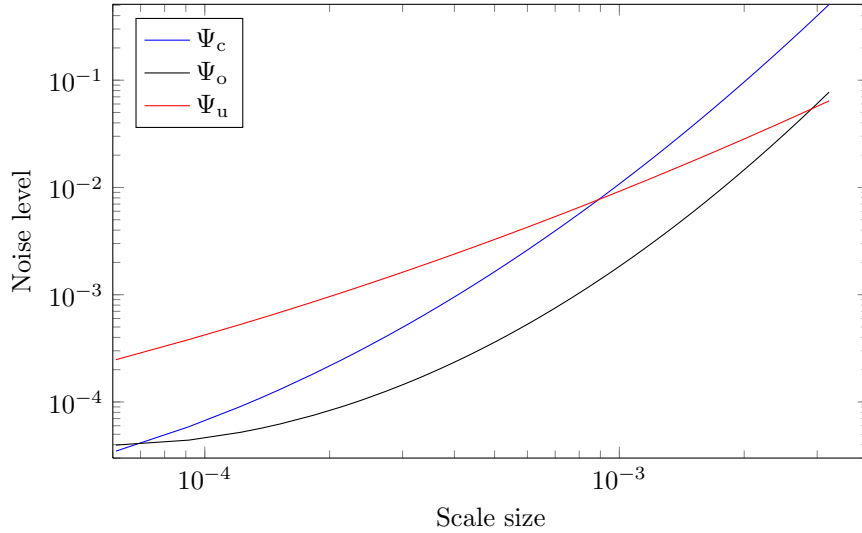


Figure 7: Upper bound for σ ensuring a 90% probability for detection of a signal of intensity 1 on the corresponding scale in the three different test setups.

4.1.3 Robustness to the noise distribution

For the correct test we furthermore investigate the empirical level using the exact variance for different data setups, cf. Table 2. We consider three scenarios:

- (1) data with Gaussian additive noise $\mathcal{N}(0, \sigma^2)$,
- (2) data with student's t additive noise $t(\nu)$ with different degrees of freedom ν ,
- (3) data with mixed Poisson and Gaussian noise.

For scenario (3) the data is generated as follows: For specified parameters $t, \sigma, b > 0$ we have

$$Y_j \stackrel{\text{independent}}{\sim} \frac{1}{t} \text{Poi}(t[(k * f)(\mathbf{x}_j) + b]) - b + \mathcal{N}(0, \sigma^2), \quad \mathbf{j} \in \{1, \dots, 512\}^2.$$

Here $\text{Poi}(\lambda)$ denotes the Poisson distribution with parameter $\lambda > 0$, and the $\mathcal{N}(0, \sigma^2)$ distribution is independent of this. This model aims for mimicking the data coming from CCD sensors (Snyder et al., 1993, 1995), modeling the (known) photon background by b , the (known) observation time by t , and the read-out errors by $\mathcal{N}(0, \sigma^2)$ with known variance $\sigma^2 > 0$.

Noise scenario	Parameters	false positive detections in %
(1)		8.8
(2)	$\nu = 3$	100
	$\nu = 6$	94.7
	$\nu = 7$	72.3
	$\nu = 11$	21.8
	$\nu = 15$	15.7
	$\nu = 19$	13.0
(3)	$\nu = 23$	13.3
	$t = 100, b = 0.5, \sigma = 0.01$	9.8
	$t = 1000, b = 0.005, \sigma = 0.01$	8.1
	$t = 100, b = 0.005, \sigma = 0.01$	14.5

Table 2: Some empirical levels computed in 1000 runs for different data settings. We always choose $\alpha = 0.1$, i.e. (asymptotically) there should $\leq 10\%$ false positives.

Note that in scenario (1) the level will be independent of σ even for finite n , because of the standardization of the local test statistics.

In conclusion we find that the heavy tail behavior of the student's t distribution strongly influences the level of the test. Note that $t(\nu)$ has $\nu - 1$ moments and hence does not satisfy (M1) for any ν . In contrast to that, in the mixture model all moments exist and satisfy (M1) whenever $b > 0$. Our simulations suggest that the test keeps its level quite stable over a large range of parameters. In the situation of a very low Poisson intensity ($t = 100, b = 0.005$), the heavier tail behavior of the Poisson distribution dominates.

4.2 Locating fluorescent markers in STED super-resolution microscopy

Based on the results from Section 4.1, we are now able to treat a real world application by identifying fluorescent markers in 2-dimensional STED (stimulated emission depletion) super-resolution microscopy (Hell and Wichmann, 1994; Klar and Hell, 1999; Hell, 2007), which allows to image samples marked by fluorescent dyes on a sub-diffraction spatial resolution.

Just as in confocal microscopy (cf. (Pawley, 2006) for an overview or (Hohage and Werner, 2016) for the mathematical treatment) the specimen is illuminated with a diffraction-limited spot for excitation. The specimen is also irradiated with a ring-like beam distribution for inhibition. This distribution prevents fluorophores from emitting fluorescence by stimulating photon emission at a longer wavelength than the ordinary one. This red-shifted emission light can be removed by a filter and hence is not seen through the microscope. Molecules that emit photons through this channel cannot emit any photons at the usual wavelength. Consequently, the light is collected from a significantly smaller region than in standard confocal microscopy, which enhances the resolution (cf. (Aspelmeier et al., 2015) for a more detailed description from a statistical perspective).

With this technique the specimen is imaged along a grid, where for each grid point several excitation pulses (say t) are applied and measured. The corresponding normalized measurements are well described by a binomial model

$$Y_{\mathbf{j}} \stackrel{\text{independent}}{\sim} \text{Bin}(t, (k * f)(\mathbf{x}_{\mathbf{j}})), \quad \mathbf{j} \in \{1, \dots, n\}^2.$$

Here $\text{Bin}(k, p)$ denotes the Binomial distribution with parameters $k \in \mathbb{N}$ and $p \in [0, 1]$, n^2 is the

number of pixels in the grid $\{\mathbf{x}_j \mid \mathbf{j} \in \{1, \dots, n\}^2\}$ and $f(\mathbf{x})$ is the probability that a photon emitted at grid point \mathbf{x} is recorded at the detector in a single excitation pulse.

The convolution kernel or point spread function (psf) can be computed by means of scalar diffraction theory (Born and Wolf, 1999) as the absolute square of the Fraunhofer diffraction pattern. In case of a circular aperture (which is the case in our experimental setup) using the paraxial approximation it simplifies to the Airy pattern

$$\mathbf{x} \mapsto \left| 2A \left(\frac{2\pi r}{\lambda} \frac{b}{f_e} \|\mathbf{x}\|_2 \right) \right|^2 \quad (25)$$

where r is the refractive index of the image space (here $r \approx 1$ for air), λ is the wavelength of the incoming light, b is the aperture radius of the exit lens and f_e its focal length. Here $A(\xi) = J_1(\xi)/\xi$ with the Bessel function J_1 of first kind. Instead of using the complicated convolution kernel in (25), we suggest to approximate the psf by a function k from the two parameter family also used in Section 4.1 by matching FWHM and kurtosis of the kernel. These values are available from measurements of the experimental psf, which yield $a = 2$ and $b = 0.016$, cf. Figure 8 for details. The plots show that these two parameters provide a remarkably good matching of the kernel functions.

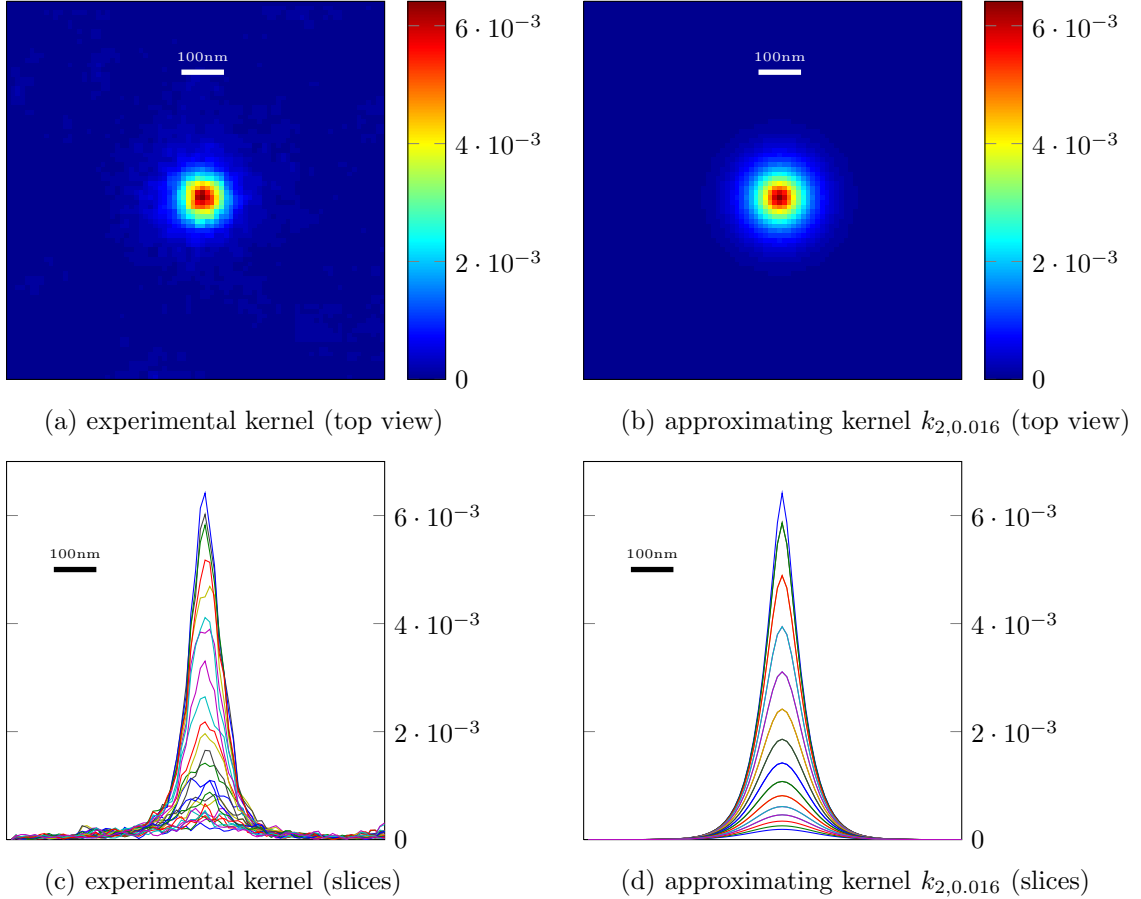


Figure 8: Experimentally measured kernel and function $k_{2,0.016}$. For the experimental kernel, we computed $\text{FWHM} = 75.9501$ nm and $\text{kurtosis} = 3.102$, and for $k_{a,b}$ we have $\text{FWHM} = 77.5881$ nm and $\text{kurtosis} = 3$.

With this kernel we design a test using the optimal probe function φ in (24) (i.e. $\beta_1 = \beta_2 = 4$) and a set of scales defined by boxes of size $k_x \times k_y$ pixels, $k_x, k_y = 4, 6, \dots, 20$. The variance used

in the test statistic is estimated from the data point-wise using a maximum likelihood estimator. Furthermore we ease the problem by neglecting all boxes in which no photons were observed, i.e. we drop all pairs $(\mathbf{t}_i, \mathbf{h}_i)$ such that $Y_{\mathbf{j}} = 0$ for all $\mathbf{x}_{\mathbf{j}} \in [\mathbf{t}_i - \mathbf{h}_i, \mathbf{t}_i]$. Even though this choice is data dependent and hence random, the uniformity over all pairs $(\mathbf{t}_i, \mathbf{h}_i)$ of our confidence statements ensures that those stay valid.

With this test we analyze the data shown in Figure 1, cf. Section 1.2 for details. For a comparison, we also use two different tests, namely an analog of MISCAT using only one single scale of size 4×6 pixels (these are the smallest boxes found by MISCAT), and a multiscale scanning test ignoring the deconvolution ($T = \text{id}$), boiling down to the test of Dümbgen and Spokoiny (2001):

$$\max_i \frac{\sqrt{\log\left(\frac{3}{\mathbf{h}_{i,1}\mathbf{h}_{i,2}}\right)}}{\log\left(\log\left(\frac{3}{\mathbf{h}_{i,1}\mathbf{h}_{i,2}}\right)\right)} \left[\frac{1}{\sqrt{\mathbf{h}_{i,1}\mathbf{h}_{i,2}}} \sum_{\mathbf{x}_{\mathbf{j}} \in [\mathbf{t}_i - \mathbf{h}_i, \mathbf{t}_i]} Y_{\mathbf{j}} - \sqrt{2 \log\left(\frac{3}{\mathbf{h}_{i,1}\mathbf{h}_{i,2}}\right)} \right].$$

For all tests we again use empirical quantiles computed in 10^4 runs of the test statistics applied to pure Gaussian white noise.

The full result is depicted in Figure 9. As mentioned in the introduction, our new test is able (at least for some of the single DNA origamis) to infer on position and rotation as indicated in Figure 9. Remarkably, this information is not clearly visible by eye, cf. Figure 2.

5 Auxiliary Results

The following theorem guarantees that the Gaussian approximation $\mathcal{S}(W)$ is asymptotically non-degenerate, bounded from below in probability and bounded from above almost surely. Recall that $(\mathbf{t}_i, \mathbf{h}_i) \in \{(\mathbf{t}_i, \mathbf{h}_i) \mid i = 1, \dots, N, \mathbf{h}_i \in (0, 1]^2, \mathbf{t}_i \in [\mathbf{h}_i, \mathbf{1}]\}$ and that, typically, $N = N(n)$ and, as $n \rightarrow \infty$, also $N(n) \rightarrow \infty$ and $h_{i,l} \rightarrow 0, l = 1, \dots, d$.

Theorem 3. *Suppose that Assumption 1 with (AHC) holds, $h_{\max} \leq n^{-\delta}$ for some $\delta > 0$. Furthermore, let Ξ be a normed function, i.e. $\int \Xi^2(\mathbf{z}) d\mathbf{z} = 1$, supported on $[0, 1]^d$. Let $Z_{\mathbf{t}, \mathbf{h}}$ and $Z_{\mathbf{t}}$ denote the fields*

$$Z_{\mathbf{t}, \mathbf{h}} := \frac{1}{\sqrt{h_1 \cdots h_d}} \int \Xi\left(\frac{\mathbf{t} - \mathbf{z}}{\mathbf{h}}\right) dW_{\mathbf{z}} \quad \text{and} \quad Z_{\mathbf{t}} = \int \Xi(\mathbf{t} - \mathbf{z}) dW_{\mathbf{z}}$$

where $W_{\mathbf{z}}$ is a standard Brownian sheet and let r_{Ξ} denote the correlation function of $Z_{\mathbf{t}}$.

(i) If r_{Ξ} is twice differentiable in zero, set

$$C_{\Xi} := (2\pi)^{-\frac{3}{2}} \sqrt{\det H_{r_{\Xi}}(\mathbf{0})}, \quad (26)$$

where $H_{r_{\Xi}}$ denotes the Hessian of r_{Ξ} .

(ii) If, for some constant $D_{\Xi} > 0$, the correlation function r_{Ξ} satisfies

$$r_{\Xi}(\mathbf{0}) = 1 - D_{\Xi} \sum_{i=1}^d |t_i| + o\left(\sum_{i=1}^d |t_i|\right), \quad \text{as } \|\mathbf{t}\| \rightarrow 0, \quad \text{set } C_{\Xi} := (2\pi)^{-\frac{1}{2}} D_{\Xi}^d.$$

(iii) For all other cases (corresponding to $\gamma \in (1/2, 1)$) set $C_{\Xi} = e$.

A) There exists a positive constant \underline{D}_{γ} such that for any fixed $\lambda \in \mathbb{R}$

$$e^{-\underline{D}_{\gamma}} e^{-\lambda} \leq \lim_{n \rightarrow \infty} \mathbb{P}(\mathcal{S}(W) \leq \lambda).$$

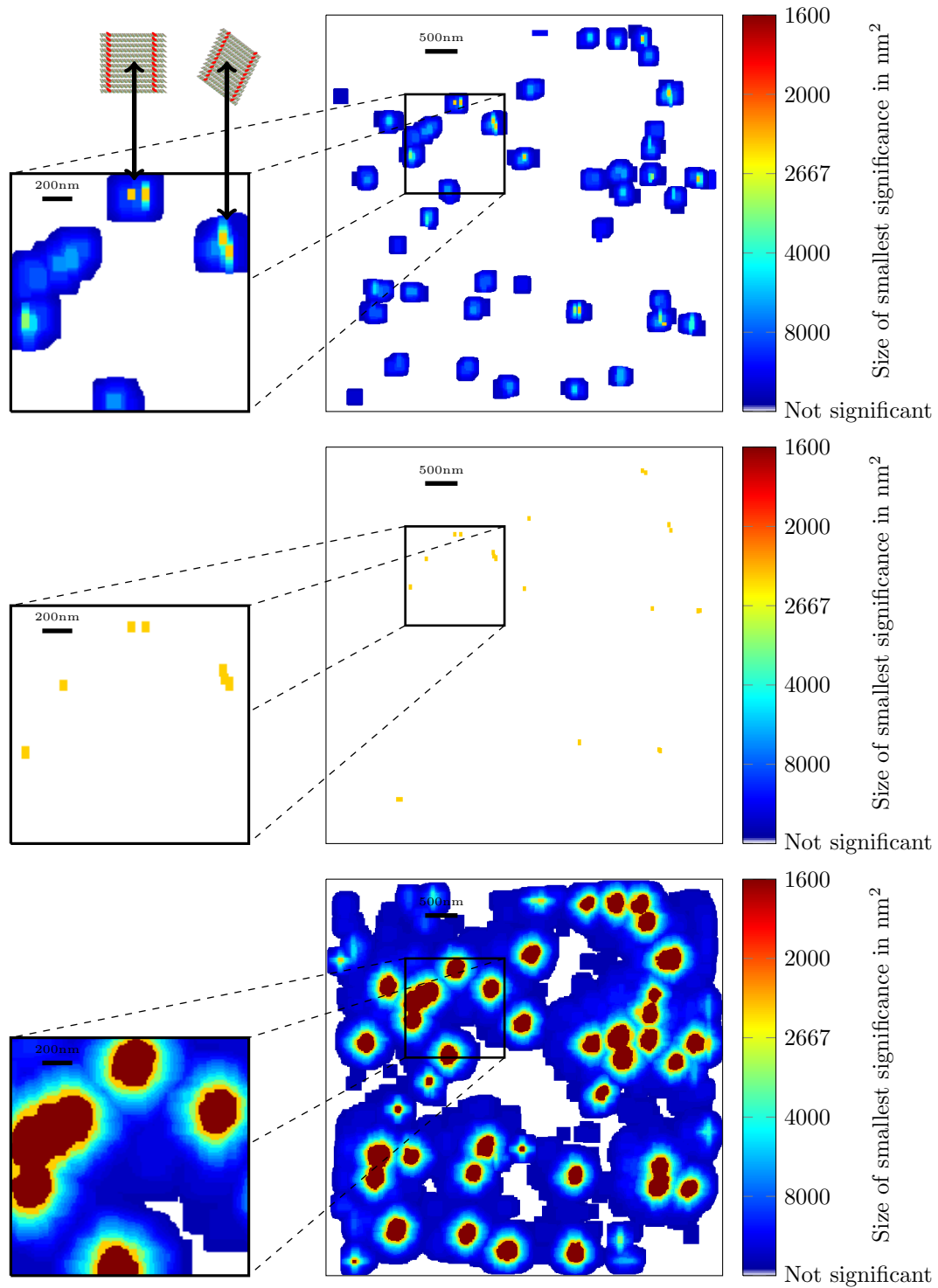


Figure 9: 90% significance maps and excerpts for different tests computed from the data in Figure 1. From top to bottom: MISCAT, a single scale test with deconvolution, and the standard multiscale test without deconvolution.

Furthermore, there exists a function F which is independent of n , such that $\lim_{\lambda \rightarrow \infty} F(\lambda) = 0$

and

$$\mathbb{P}(\mathcal{S}(W) > \lambda) \leq F(\lambda).$$

This implies in particular that $\mathcal{S}(W)$ is almost surely bounded.

B) If (14) and (15) hold and if either r_{Ξ} is twice differentiable in zero or Assumption (AHCb) holds, we have the following upper bound on the distribution function of $\mathcal{S}(W)$ for some positive constant \bar{D}_{γ}

$$\lim_{n \rightarrow \infty} \mathbb{P}(\mathcal{S}(W) \leq \lambda) \leq e^{-\bar{D}_{\gamma} e^{-\lambda}},$$

where $C_d = 2d + d/\gamma - 1$ and $\omega_i(C_{\Xi}, C_d)$ is defined in (13).

Corollary 1 below follows immediately from the proof of the previous Theorem. Two special cases are discussed in Remark 2.

Corollary 1. *Suppose that the assumptions of Theorem 3 hold. Replace Assumption (15) as follows. Assume that $\mathbf{h}_i \in \mathcal{H}_1 \times \dots \times \mathcal{H}_d$, where possibly $\mathcal{H}_i \neq \mathcal{H}_j$ for $i \neq j$. Let for $\mathcal{P} := \{\lfloor \log(1/h_{\max}) \rfloor - 2, \lfloor \log(1/h_{\max}) \rfloor - 1, \dots, \lfloor \log(1/h_{\min}) \rfloor\}$, and $j \in \{1, \dots, d\}$*

$$\mathcal{P}_j := \{p \in \mathcal{P} \mid \exists h_{i,j} \in \mathcal{H}_j : 1/h_{i,j} \in (e^p, e^{(p+1)})\}.$$

Then, if the constant C_d is chosen such that there exist positive constants \underline{d} and \bar{D} such that

$$\underline{d} \leq \left(\frac{1}{\log(n)} \right)^{\frac{C_d - d/\gamma + 1}{2}} |\mathcal{P}_1 \times \dots \times \mathcal{P}_d| \leq \bar{D},$$

the results of Theorem 3 remain valid.

6 Proofs

Throughout the proofs the letter C without a subscript denotes a generic, positive constant whose value may vary from line to line.

We will first prove the auxiliary results from Section 5, as they are needed for the proofs of the main results.

Proof of Theorem 3. For ease of notation we give a detailed proof for the case $d = 2$. Since the problem basically factorizes into two one-dimensional problems after the first steps, it is obvious how to carry over the ideas and techniques of this proof to a higher dimensional setting. All results that are used throughout the proof hold for general dimension d . A first observation, which is crucial to all what follows, is that, due to the convolution structure, the process $Z_{t, \mathbf{h}}$ is stationary for a fixed \mathbf{h} .

Step I: The lower bound

We now prove the first part of the assertion of the theorem. To this end we "reduce" the set of scales to the "relevant" ones by a slicing technique.

Step I.1: Reduction of the set of scales by slicing

Let $D > 0$ be a positive constant and define, for $p \in \mathcal{P}_D := \{\lfloor \log(1/h_{\max})/D \rfloor - 2, \lfloor \log(1/h_{\max})/D \rfloor - 1, \dots, \lfloor \log(1/h_{\min})/D \rfloor\}$, the intervals

$$I_{p,D} := \left(e^{Dp}, e^{D(p+1)} \right], \quad p \in \mathcal{P}_D. \quad (27)$$

Obviously, we have

$$\left(\frac{1}{h_{\max}}, \frac{1}{h_{\min}} \right] \subset \bigcup_{p \in \mathcal{P}_D} I_{p,D}.$$

Let $h_{p,D} = h_p := \exp(-D(p+1))$ denote the smallest scale such that $1/h \in I_{p,D}$. Then

$$\begin{aligned}
& \max_{i \in \{1, \dots, N\}} \omega_{\mathbf{h}_i}(Z_{\mathbf{t}_i, \mathbf{h}_i} - \omega_{\mathbf{h}_i}) \stackrel{\mathcal{D}}{=} \max_{p, q \in \mathcal{P}_D} \max_{\mathbf{h} \in I_p \times I_q} \sup_{\mathbf{t} \in [1, 1/h_p] \times [1, 1/h_q]} \omega_{\mathbf{h}}(Z_{\mathbf{t}} - \omega_{\mathbf{h}}) \\
& \leq \max_{p, q \in \mathcal{P}_D} \sup_{\mathbf{t} \in [1, 1/h_p] \times [1, 1/h_q]} \omega_{(h_p, h_q)}(Z_{\mathbf{t}} - \omega_{(h_p, h_q)}) \\
& \quad + \frac{C}{\sqrt{\log(n)}} \left| \max_{p, q \in \mathcal{P}_D} \sup_{\mathbf{t} \in [h_p, 1] \times [h_q, 1]} \omega_{(h_p, h_q)}(Z_{\mathbf{t}} - \omega_{(h_p, h_q)}) \right| + 2D + o(1), \tag{28}
\end{aligned}$$

where the estimate is deterministic and holds everywhere. Notice that we replaced the discrete grid for the parameter \mathbf{t} by the corresponding rectangle, which gives an upper bound. Hence, we only consider the representative scales h_p , $p \in \mathcal{P}_D$ and define the set $\mathcal{H}_D := \{h_p \mid p \in \mathcal{P}_D\}$. Let

$$\begin{aligned}
& \max_{\mathbf{h} \in \mathcal{H}_D^2} \sup_{\mathbf{t} \in [h, 1]} \omega_{\mathbf{h}} \left(\frac{1}{\sqrt{h_1 h_2}} \int \Xi \left(\frac{\mathbf{t} - \mathbf{z}}{\mathbf{h}} \right) dW_{\mathbf{z}} - \omega_{\mathbf{h}} \right) \\
& \stackrel{\mathcal{D}}{=} \max_{\mathbf{h} \in \mathcal{H}_D^2} \sup_{\mathbf{t} \in [1, 1/h]} \omega_{\mathbf{h}} \left(\int \Xi(\mathbf{t} - \mathbf{z}) dW_{\mathbf{z}} - \omega_{\mathbf{h}} \right) =: M_n, \tag{29}
\end{aligned}$$

by stationarity of $Z_{\mathbf{t}, \mathbf{h}}$ for fixed \mathbf{h} . We now consider the term M_n and incorporate the error estimates into the result in Step III below.

Step I.2: Partition of the parameter set

The form of M_n in (29) reveals a redundancy pattern that we will exploit later on. Observe that the suprema with respect to \mathbf{t} of the rescaled version M_n are taken over subsets of the rectangle $[1, 1/h_{\min}]$. For smaller scales, the supremum with respect to \mathbf{t} is taken over larger sets. Obviously, for $(p, q) \in \mathcal{P}_D^2$,

$$[1/h_p, 1/h_{p+1}] \times [1/h_q, 1/h_{q+1}] \subset [1, 1/h_r] \times [1, 1/h_s] \quad \forall \quad r > p+1, s > q+1.$$

In order to exploit this fact we partition the parameter set $[1, 1/h_{\min}]$ into suitable blocks, i.e. into blocks $B_{p+1, q+1}$ that are approximately equal to $[1/h_p, 1/h_{p+1}] \times [1/h_q, 1/h_{q+1}]$ in order to split the suprema w.r.t \mathbf{t} into suitable sub-suprema. To achieve that those sub-suprema are independent, we separate the blocks by small bands of width 1 and separate those by unit-cubes (see Figure 10). This ensures independence, since $\text{supp}(\Xi) \subset [0, 1]^d$. The bands and cubes only yield a contribution which is asymptotically negligible.

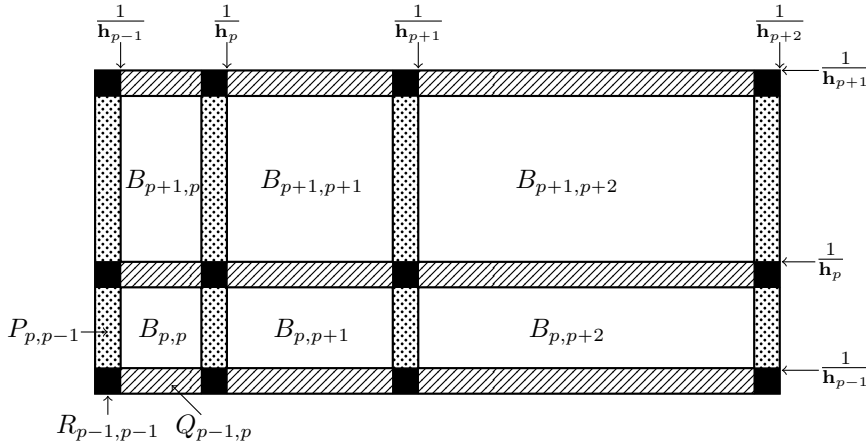


Figure 10: Detail of the partition of the set $[1, 1/h_{\min}] \times [1, 1/h_{\min}]$.

To be precise, we define subsets of $[1, 1/h_{\min}] \times [1, 1/h_{\min}]$ as follows

$$\begin{aligned} B_{i,j} &:= \left[\frac{1}{h_{i-1}}, \frac{1}{h_i} - 1 \right) \times \left[\frac{1}{h_{j-1}}, \frac{1}{h_j} - 1 \right), \quad R_{i,j} := \left[\frac{1}{h_i} - 1, \frac{1}{h_i} \right) \times \left[\frac{1}{h_j} - 1, \frac{1}{h_j} \right), \\ Q_{i,j} &:= \left[\frac{1}{h_{i-1}}, \frac{1}{h_i} - 1 \right) \times \left[\frac{1}{h_j} - 1, \frac{1}{h_j} \right), \quad \text{and } P_{i,j} := \left[\frac{1}{h_i} - 1, \frac{1}{h_i} \right) \times \left[\frac{1}{h_{j-1}}, \frac{1}{h_j} - 1 \right). \end{aligned} \quad (30)$$

Figure 10 shows a detail of the partition. The large blocks $B_{i,j}$ yield the main contributions. The blocks $Q_{i,j}$ (shaded) and $P_{i,j}$ (dotted) separate the $B_{i,j}$ and are separated by the smallest blocks, $R_{i,j}$ (black). Furthermore, define

$$\mathcal{B}_{k,l} := \bigcup_{\substack{i \in \mathcal{P}_D, i \leq k \\ j \in \mathcal{P}_D, j \leq l}} B_{i,j}, \quad \mathcal{P}_{k,l} := \bigcup_{\substack{i \in \mathcal{P}_D, i \leq k \\ j \in \mathcal{P}_D, j \leq l}} P_{i,j}, \quad \mathcal{Q}_{k,l} := \bigcup_{\substack{i \in \mathcal{P}_D, i \leq k \\ j \in \mathcal{P}_D, j \leq l}} Q_{i,j}, \quad \text{and } \mathcal{R}_{k,l} := \bigcup_{\substack{i \in \mathcal{P}_D, i \leq k \\ j \in \mathcal{P}_D, j \leq l}} R_{i,j},$$

$$M_{\mathcal{B}_{k,l}} := \sup_{\mathbf{t} \in \mathcal{B}_{k,l}} \int \Xi(\mathbf{t} - \mathbf{z}) dW_{\mathbf{z}},$$

and define $M_{\mathcal{P}_{k,l}}$, $M_{\mathcal{Q}_{k,l}}$ and $M_{\mathcal{R}_{k,l}}$ accordingly. Write

$$M_n = \max_{(k,l) \in \mathcal{P}_D^2} \omega_{(h_k, h_l)} \left(\max\{M_{\mathcal{B}_{k,l}}, M_{\mathcal{P}_{k,l}}, M_{\mathcal{Q}_{k,l}}, M_{\mathcal{R}_{k,l}}\} - \omega_{(h_k, h_l)} \right)$$

and notice that, for $\lambda \in \mathbb{R}$,

$$\begin{aligned} &\mathbb{P} \left(\max_{(k,l) \in \mathcal{P}_D^2} \omega_{(h_k, h_l)} \left(\max\{M_{\mathcal{B}_{k,l}}, M_{\mathcal{P}_{k,l}}, M_{\mathcal{Q}_{k,l}}, M_{\mathcal{R}_{k,l}}\} - \omega_{(h_k, h_l)} \right) \leq \lambda \right) \\ &\geq \mathbb{P} \left(\max_{(k,l) \in \mathcal{P}_D^2} \omega_{(h_k, h_l)} \left(M_{\mathcal{B}_{k,l}} - \omega_{(h_k, h_l)} \right) \leq \lambda \right) \cdot \mathbb{P} \left(M_{\mathcal{B}_{k,l}} > \max\{M_{\mathcal{P}_{k,l}}, M_{\mathcal{Q}_{k,l}}, M_{\mathcal{R}_{k,l}}\} \forall k, l \right). \end{aligned}$$

We have that

$$\begin{aligned} &\mathbb{P} \left(M_{\mathcal{B}_{k,l}} > \max\{M_{\mathcal{P}_{k,l}}, M_{\mathcal{Q}_{k,l}}, M_{\mathcal{R}_{k,l}}\} \forall k, l \right) \\ &\geq 1 - \sum_{(k,l) \in \mathcal{P}_D^2} \left(\mathbb{P} \left(M_{\mathcal{B}_{k,l}} \leq M_{\mathcal{P}_{k,l}} \right) + \mathbb{P} \left(M_{\mathcal{B}_{k,l}} \leq M_{\mathcal{Q}_{k,l}} \right) + \mathbb{P} \left(M_{\mathcal{B}_{k,l}} \leq M_{\mathcal{R}_{k,l}} \right) \right). \end{aligned}$$

We now estimate the term $\mathbb{P} \left(M_{\mathcal{B}_{k,l}} \leq M_{\mathcal{P}_{k,l}} \right)$. The terms $\mathbb{P} \left(M_{\mathcal{B}_{k,l}} \leq M_{\mathcal{Q}_{k,l}} \right)$ and $\mathbb{P} \left(M_{\mathcal{B}_{k,l}} \leq M_{\mathcal{R}_{k,l}} \right)$ can be estimated analogously. We use that $\mathbb{E}[M_{\mathcal{B}_{k,l}}] \sim \sqrt{2 \log(1/(h_k h_l))}$, whereas $\mathbb{E}[M_{\mathcal{P}_{k,l}}] \sim \sqrt{2 \log(1/(h_k))}$ so that $\sqrt{2 \log(1/(h_k \sqrt{h_l}))}$ overestimates the expectation of $M_{\mathcal{P}_{k,l}}$ but underestimates the expectation of $M_{\mathcal{B}_{k,l}}$. We obtain

$$\begin{aligned} &\mathbb{P} \left(M_{\mathcal{B}_{k,l}} \leq M_{\mathcal{P}_{k,l}} \right) \leq \mathbb{P} \left(M_{\mathcal{P}_{k,l}} > \sqrt{2 \log(1/(h_k \sqrt{h_l}))} \right) + \mathbb{P} \left(M_{\mathcal{B}_{k,l}} < \sqrt{2 \log(1/(h_k \sqrt{h_l}))} \right) \\ &\leq C \left(\mathbb{P} \left(\sup_{\mathbf{t} \in \mathcal{P}_{k,l}} \int \Xi(\mathbf{t} - \mathbf{z}) dW_{\mathbf{z}} > \sqrt{2 \log(1/(h_k \sqrt{h_l}))} \right) \right. \\ &\quad \left. + \mathbb{P} \left(\sup_{\mathbf{t} \in \mathcal{B}_{k,l}} \int \Xi(\mathbf{t} - \mathbf{z}) dW_{\mathbf{z}} < \sqrt{2 \log(1/(h_k \sqrt{h_l}))} \right) \right) \\ &\leq C \left(\sqrt{h_l} + \mathbb{P} \left(\sup_{\mathbf{t} \in \mathcal{B}_{k,l}} \int \Xi(\mathbf{t} - \mathbf{z}) dW_{\mathbf{z}} < \sqrt{2 \log(1/(h_k \sqrt{h_l}))} \right) \right), \end{aligned}$$

where we applied Borell's inequality. Since

$$\sqrt{2 \log(1/(h_k \sqrt{h_l}))} < \mathbb{E} \left[\sup_{\mathbf{t} \in \mathcal{B}_{k,l}} \int \Xi(\mathbf{t} - \mathbf{z}) dW_{\mathbf{z}} \right] - \tau_1 \sqrt{\log(n)},$$

for some $\tau_1 > 0$, Borell's inequality gives

$$\mathbb{P}\left(M_{\mathcal{B}_{k,l}} \leq M_{\mathcal{P}_{k,l}}\right) \leq C \sum_{(k,l) \in \mathcal{P}_D^2} \left(\sqrt{h_l} + n^{-\frac{\tau_1}{2}}\right) \leq C \log(n)^2 \left(n^{-\frac{\delta}{2}} + n^{-\frac{\tau_1}{2}}\right).$$

The last estimate follows from Assumption (G). Hence, there exists a constant $\tau > 0$ such that

$$\mathbb{P}\left(\max_{(i,j) \in \mathcal{P}_D^2} \omega_{(h_i, h_j)} \left(\max\{M_{\mathcal{B}_{k,l}}, M_{\mathcal{P}_{k,l}}, M_{\mathcal{Q}_{k,l}}, M_{\mathcal{R}_{k,l}}\} - \omega_{(h_i, h_j)}\right) \leq \lambda\right) \geq \mathbb{P}\left(M_{\mathcal{B}} \leq \lambda\right) \cdot \left(1 - \frac{C}{n^\tau}\right),$$

where $M_{\mathcal{B}} := \max_{(k,l) \in \mathcal{P}_D^2} \omega_{(h_k, h_l)} \left(M_{\mathcal{B}_{k,l}} - \omega_{(h_k, h_l)}\right)$. In order to establish the lower bound, it remains to consider the term $M_{\mathcal{B}}$. Write

$$\begin{aligned} M_{\mathcal{B}} &= \max_{(i,j) \in \mathcal{P}_D^2} \max_{(k,l) \leq (i,j)} \sup_{\mathbf{t} \in B_{k,l}} \omega_{(h_i, h_j)} \left(\int \Xi(\mathbf{t} - \mathbf{z}) dW_{\mathbf{z}} - \omega_{(h_i, h_j)}\right) \\ &= \max_{(k,l) \in \mathcal{P}_D^2} \max_{(k,l) \leq (i,j)} \sup_{\mathbf{t} \in B_{k,l}} \omega_{(h_i, h_j)} \left(\int \Xi(\mathbf{t} - \mathbf{z}) dW_{\mathbf{z}} - \omega_{(h_i, h_j)}\right). \end{aligned}$$

Fix $\lambda \in \mathbb{R}$. The blocks $B_{k,l}$ are constructed such that the sub-maxima over different blocks are independent. This yields

$$\begin{aligned} \mathbb{P}(M_{\mathcal{B}_{k,l}} \leq \lambda) &= \prod_{(k,l) \in \mathcal{P}_D^2} \mathbb{P}\left(\max_{(k,l) \leq (i,j)} \sup_{\mathbf{t} \in B_{k,l}} \omega_{(h_i, h_j)} \left(\int \Xi(\mathbf{t} - \mathbf{z}) dW_{\mathbf{z}} - \omega_{(h_i, h_j)}\right) \leq \lambda\right) \\ &= \prod_{(k,l) \in \mathcal{P}_D^2} \mathbb{P}\left(\sup_{\mathbf{t} \in B_{k,l}} \int \Xi(\mathbf{t} - \mathbf{z}) dW_{\mathbf{z}} \leq \Lambda_{\min, k, l}\right), \end{aligned}$$

where

$$\Lambda_{\min, k, l} := \min_{(k,l) \leq (i,j)} \left(\frac{\lambda}{\omega_{(h_i, h_j)}} + \omega_{(h_i, h_j)}\right).$$

Now we have broken the proof down into $|\mathcal{P}_D|^2$ "one-scale" extreme value problems and use standard results for those. Let $\text{Leb}(B_{k,l})$ denote the Lebesgue-measure of $B_{k,l}$ and let $\Lambda_{k,l}$ denote

$$\Lambda_{k,l} := \frac{\lambda}{\omega_{(h_k, h_l)}} + \omega_{(h_k, h_l)}. \quad (31)$$

By Theorem 4.1.2 in (Adler and Taylor, 2007) we deduce that there exists a constant $D_{\gamma,1}$, depending only on the degree of average Hölder smoothness, γ , (see (AHC) in Assumption 1) such that

$$\begin{aligned} \mathbb{P}(M_{\mathcal{B}_{k,l}} \leq \lambda) &\geq \prod_{(k,l) \in \mathcal{P}_D^2} \left(1 - D_{\gamma,1} \text{Leb}(B_{k,l}) \Lambda_{\min, k, l}^{d/\gamma-1} \exp\left(-\frac{1}{2} \Lambda_{\min, k, l}^2\right)\right) \\ &\geq \prod_{(k,l) \in \mathcal{P}_D^2} \left(1 - D_{\gamma,1} \text{Leb}(B_{k,l}) \Lambda_{k,l}^{d/\gamma-1} \exp\left(-\frac{1}{2} \Lambda_{\min, k, l}^2\right)\right), \end{aligned}$$

since $\Lambda_{\min, k, l} \leq \Lambda_{k,l}$. Also, $\Lambda_{\min, k, l} = \left(\frac{\lambda}{\omega_{(h_{i_0}, h_{j_0})}} + \omega_{(h_{i_0}, h_{j_0})}\right)$ for some $(k, l) \leq (i_0, j_0)$. Hence, $\Lambda_{\min, k, l}^2 = (\lambda/(\omega_{(h_{i_0}, h_{j_0})}))^2 + 2\lambda + \omega_{(h_{i_0}, h_{j_0})}^2 \geq 2\lambda + \omega_{(h_k, h_l)}^2$, where we used that $h_p > h_{p+1} \forall p \in \mathcal{P}_D$. We obtain

$$\mathbb{P}(M_{\mathcal{B}_{k,l}} \leq \lambda) \geq \prod_{(k,l) \in \mathcal{P}_D^2} \left(1 - C \text{Leb}(B_{k,l}) h_k h_l e^{-\lambda} \left(\left(\frac{\lambda^2}{2 \log\left(\frac{C_{\Xi}}{h_k h_l}\right)}\right)^{\frac{d}{2\gamma}-\frac{1}{2}} + \omega_{k,l}^{\frac{d}{\gamma}-1}\right) \left(\frac{1}{\log\left(\frac{C_{\Xi}}{h_k h_l}\right)}\right)^{\frac{C_d}{2}}\right).$$

We find, for sufficiently large n ,

$$\begin{aligned} \mathbb{P}(M_{\mathcal{B}_{k,l}} \leq \lambda) &\geq \prod_{(k,l) \in \mathcal{P}_D^2} \left(1 - C \frac{e^{D-1}}{e^{2D}} e^{-\lambda} \left(\frac{1}{2 \log(C_{\Xi}/(h_k h_l))} \right)^{\frac{C_d}{2}} \left(\left(\frac{\lambda^2}{2 \log(\frac{C_{\Xi}}{h_k h_l})} \right)^{\frac{d}{2\gamma} - \frac{1}{2}} + \omega_{k,l}^{\frac{d}{\gamma} - 1} \right) \right) \\ &\geq \exp \left(\sum_{(k,l) \in \mathcal{P}_D^2} \log \left(1 - C e^{-\lambda} \left(\frac{1}{2 \log(C_{\Xi}/(h_k h_l))} \right)^{\frac{C_d - d/\gamma + 1}{2}} + \left(\frac{|\lambda|^{\frac{d}{\gamma} - 1}}{(2 \log(C_{\Xi}/(h_k h_l)))^{\frac{C_d + d/\gamma - 1}{2}}} \right) \right) \right). \end{aligned}$$

Recall that $C_d = 2d + d/\gamma - 1$ and hence $\frac{C_d - d/\gamma + 1}{2} = d = 2$ as well as $\frac{C_d + d/\gamma - 1}{2} \geq 2d - 1$. Notice that there exists a constant $\mathcal{C} > 0$ such that

$$0 \leq C e^{-\lambda} \left(\frac{1}{2 \log(C_{\Xi}/(h_k h_l))} \right)^2 + \left(\frac{|\lambda|}{2 \log(C_{\Xi}/(h_k h_l))} \right)^{\frac{5}{2}} \leq \mathcal{C} / \log(n)^2 \leq \frac{1}{2},$$

for all k and l and for sufficiently large n . We now apply the inequality $\log(1 - x) \geq -2x$, which holds, in particular, for all $x \in [0, 0.5]$.

$$\mathbb{P}(M_{\mathcal{B}_{k,l}} \leq \lambda) \geq \exp \left(-C e^{-\lambda} \sum_{(k,l) \in \mathcal{P}_D^2} \left(\left(\frac{1}{2 \log(C_{\Xi}/(h_k h_l))} \right)^2 + \left(\frac{|\lambda|^{\frac{d}{\gamma} - 1}}{(2 \log(C_{\Xi}/(h_k h_l)))^{2d-1}} \right) \right) \right)$$

Recall that $h_p = \exp(-D(p+1))$, which yields

$$\begin{aligned} \mathbb{P}(M_{\mathcal{B}_{k,l}} \leq \lambda) &\geq \exp \left(-C e^{-\lambda} \sum_{(k,l) \in \mathcal{P}_D^2} \left(\left(\frac{1}{2(\log(C_{\Xi}) + Dk + Dl + 2D)} \right)^2 \right. \right. \\ &\quad \left. \left. + \left(\frac{|\lambda|}{2(\log(C_{\Xi}) + Dk + Dl + 2D)} \right)^{\frac{5}{2}} \right) \right). \end{aligned}$$

The sum $\sum_{(k,l) \in \mathcal{P}_D^2} \frac{1}{(k+l)^2}$ is bounded above (in n) since

$$\sum_{(k,l) \in \mathcal{P}_D^2} \frac{1}{(k+l)^2} \leq \frac{|\mathcal{P}_D|^2}{(2 \min \mathcal{P}_D)^2} \leq \frac{|\log(1/h_{\min})/D - \lfloor \log(1/h_{\max})/D \rfloor + 2|^2}{(|\log(1/h_{\max})/D - 2|^2)} \leq \frac{(\log(n) + 2D)^2}{(\delta \log(n) - 3D)^2}.$$

Hence,

$$\mathbb{P}(M_{\mathcal{B}_{k,l}} \leq \lambda) \geq \exp \left(-C e^{-\lambda} \left(1 + \frac{|\lambda|^{\frac{d}{\gamma} - 1}}{\sqrt{\log(n)}} \right) \right)$$

This completes the proof for the lower bound.

Step II: An upper bound

Step II.1: Reduction of the set of scales

Since all scales are considered, none of the intervals I_p are empty. We proceed here as in Step I.1 and find

$$\begin{aligned} \max_{i \in \{1, \dots, N\}} \omega_{\mathbf{h}_i} (Z_{\mathbf{t}_i, \mathbf{h}_i} - \omega_{\mathbf{h}_i}) &\geq \max_{p, q \in \mathcal{P}_D^2} \sup_{\mathbf{t} \in [h_p, 1] \times [h_q, 1]} \omega_{(h_p, h_q)} (Z_{\mathbf{t}} - \omega_{(h_p, h_q)}) \\ &\quad - \frac{C}{\sqrt{\log(n)}} \left| \max_{p, q \in \mathcal{P}_D^2} \sup_{\mathbf{t} \in [h_p, 1] \times [h_q, 1]} \omega_{(h_p, h_q)} (Z_{\mathbf{t}} - \omega_{(h_p, h_q)}) \right| - 2D - o(1). \end{aligned} \tag{32}$$

Step II.2: Replacement of the discrete parameter sets of \mathbf{t} by intervals

We now show that the grids $\{(t_{i,1}/h_{i,1}, t_{i,2}/h_{i,2}) \mid 1 \leq i \leq N\} =: \frac{1}{\mathbf{h}_i} \mathcal{T}_{\mathbf{h}_i}$ can be replaced by the rectangles $[\mathbf{1}, \mathbf{1}/\mathbf{h}_i]$. To this end let $p \in \mathbb{N}$ be even and let $(p-1)!!$ denote the product

$$(p-1)!! = (p-1) \cdot (p-3) \cdot \dots \cdot 3 \cdot 1.$$

Then, by (AHC), for any $p \in 2\mathbb{N}$,

$$\begin{aligned} \mathbb{E} \left(\int \Xi(\mathbf{t} - \mathbf{z}) dW_{\mathbf{z}} - \int \Xi(\mathbf{s} - \mathbf{z}) dW_{\mathbf{z}} \right)^p &= (p-1)!! \left(\mathbb{E} \left(\int (\Xi(\mathbf{t} - \mathbf{z}) - \Xi(\mathbf{s} - \mathbf{z})) dW_{\mathbf{z}} \right)^2 \right)^{\frac{p}{2}} \\ &= (p-1)!! \left(\int (\Xi(\mathbf{t} - \mathbf{z}) - \Xi(\mathbf{s} - \mathbf{z}))^2 d\mathbf{z} \right)^{\frac{p}{2}} \leq (p-1)!! L_{\Xi}^p \|\mathbf{t} - \mathbf{s}\|_{l^2}^{\gamma p}. \end{aligned}$$

Hence, by Theorem 2.5.1 in (Khoshnevisan, 2002), for all $\gamma \in [1/2, 1]$ there exists a modification $\{Z_{\mathbf{t}} \mid \mathbf{t} \in \mathbb{R}_+^d\}$ which is Hölder-continuous of any order $\gamma_H < 1/2$. Without loss of generality, $\|\mathbf{t}_i - \mathbf{t}_j\|_{\infty} \leq 1/n$. We find, for sufficiently large n ,

$$\begin{aligned} &\mathbb{P} \left(\max_{\mathbf{h} \in \mathcal{H}_D^2} \omega_{\mathbf{h}} \left(\max_{\mathbf{t} \in \frac{1}{\mathbf{h}} \mathcal{T}_{\mathbf{h}}} Z_{\mathbf{t}} - \omega_{\mathbf{h}} \right) \leq \lambda \right) \\ &\leq \mathbb{P} \left(\max_{\mathbf{h} \in \mathcal{H}_D^2} \omega_{\mathbf{h}} \left(\max_{\mathbf{t} \in [1, 1/\mathbf{h}]} Z_{\mathbf{t}} - \omega_{\mathbf{h}} \right) - \max_{\mathbf{h}} \omega_{\mathbf{h}} \sup_{\mathbf{s}, \mathbf{t}: \|\mathbf{s} - \mathbf{t}\|_{l^2} \leq \frac{\sqrt{2}}{nh_{\min}}} |Z_{\mathbf{t}} - Z_{\mathbf{s}}| \leq \lambda \right), \end{aligned}$$

where $\max_{\mathbf{h}} \omega_{\mathbf{h}} \sup_{\mathbf{s}, \mathbf{t}: \|\mathbf{s} - \mathbf{t}\|_{l^2} \leq \frac{\sqrt{2}}{nh_{\min}}} |Z_{\mathbf{t}} - Z_{\mathbf{s}}|$ is the maximal error that can occur when the grid $\frac{1}{\mathbf{h}_i} \mathcal{T}_{\mathbf{h}_i}$ is replaced by the rectangle $[1, 1/\mathbf{h}]$. Now we use Assumption (SR) and obtain, by Hölder continuity of $Z_{\mathbf{t}}$,

$$\begin{aligned} &\mathbb{P} \left(\max_{\mathbf{h} \in \mathcal{H}_D^2} \omega_{\mathbf{h}} \left(\max_{\mathbf{t} \in [1, 1/\mathbf{h}] \cap \frac{1}{nh_1} \mathbb{N} \times \frac{1}{nh_2} \mathbb{N}} Z_{\mathbf{t}} - \omega_{\mathbf{h}} \right) \leq \lambda \right) \\ &\leq \mathbb{P} \left(\max_{\mathbf{h} \in \mathcal{H}_D^2} \omega_{\mathbf{h}} \left(\max_{\mathbf{t} \in [1, 1/\mathbf{h}]} Z_{\mathbf{t}} - \omega_{\mathbf{h}} \right) - \omega_{(h_{\min}, h_{\min})} C \left(\frac{\sqrt{2}}{nh_{\min}} \right)^{\gamma_H} \leq \lambda \right) \\ &\leq \mathbb{P} \left(\max_{\mathbf{h} \in \mathcal{H}_D^2} \omega_{\mathbf{h}} \left(\max_{\mathbf{t} \in [1, 1/\mathbf{h}]} Z_{\mathbf{t}} - \omega_{\mathbf{h}} \right) \leq \lambda + \frac{1}{\sqrt{\log(n)}} \right). \end{aligned}$$

Step II.3: Partition of the parameter set

We consider the same partition as in the proof for the lower bound (see (30)). The small blocks, however, can be discarded as this gives an upper bound, i.e.:

$$\mathbb{P} \left(\max_{\mathbf{h} \in \mathcal{H}_D^2} \omega_{\mathbf{h}} \left(\max_{\mathbf{t} \in [1, 1/\mathbf{h}]} Z_{\mathbf{t}} - \omega_{\mathbf{h}} \right) \leq \lambda \right) \leq \mathbb{P} \left(\max_{\mathbf{h} \in \mathcal{H}_D^2} \omega_{\mathbf{h}} \left(\max_{\mathbf{t} \in \mathcal{B}} Z_{\mathbf{t}} - \omega_{\mathbf{h}} \right) \leq \lambda \right).$$

Step II.4: An upper bound for the case $\gamma = 1$

In the case $\gamma = 1$, Gaussian comparison to a smoother process yields an upper bound which is sharp. To this end, let $\hat{\Xi}$ a smooth function such that $r_{\hat{\Xi}}$ is integrable, $r_{\hat{\Xi}}(\mathbf{0}) = r_{\Xi}(\mathbf{0})$ and $r_{\hat{\Xi}}(\mathbf{t}) \geq r_{\Xi}(\mathbf{t})$ for all $\mathbf{t} \in \mathbb{R}^2$. Then, by Slepian's inequality

$$\mathbb{P} \left(\sup_{\mathbf{t} \in B_{k,l}} \int \Xi(\mathbf{t} - \mathbf{z}) dW_{\mathbf{z}} \leq \Lambda_{k,l} \right) \leq \mathbb{P} \left(\sup_{\mathbf{t} \in B_{k,l}} \int \hat{\Xi}(\mathbf{t} - \mathbf{z}) dW_{\mathbf{z}} \leq \Lambda_{k,l} \right)$$

Define

$$\hat{\omega}_{k,l,\hat{\Xi}} := \sqrt{2 \log(C_{\hat{\Xi}} \text{Leb}(B_{k,l}))} + C_d \frac{\log(2 \log(C_{\hat{\Xi}} \text{Leb}(B_{k,l})))}{2\sqrt{2 \log(C_{\hat{\Xi}} \text{Leb}(B_{k,l}))}}.$$

Choose D in (27) such that $C_{\hat{\Xi}} \text{Leb}(B_{k,l}) = C_{\Xi}/(h_k h_l)$. Then, by Theorem 14.2 in (Piterbarg, 1996), we deduce

$$\begin{aligned} \mathbb{P}(M_{B_{k,l}} \leq \lambda) &\leq \prod_{(k,l) \in \mathcal{P}_D^2} \mathbb{P} \left(\sup_{\mathbf{t} \in B_{k,l}} \int \hat{\Xi}(\mathbf{t} - \mathbf{z}) dW_{\mathbf{z}} \leq \Lambda_{k,l} \right) \\ &\leq \exp \left(- \exp(-\lambda - C\lambda^2/\log(n)) \left(1 + \frac{\lambda}{\omega_{k,l}}\right) \sum_{(k,l) \in \mathcal{P}_D^2} \left(\frac{1}{2 \log(C_{\Xi}/(h_k h_l))} \right)^{\frac{C_d - d + 1}{2}} \right) (1 + O(n^{-\tau})), \end{aligned}$$

for some $\tau > 0$. Since we consider the case $\gamma = 1$, we have that $C_d/2 - d/2 + 1/2 = d = 2$. As in Step I.2, we plug in the definition of h_k and h_l . This yields, for a positive constant $C_{\Xi, D}$

$$\mathbb{P}(M_{\mathcal{B}_{k,l}} \leq \lambda) \leq \exp\left(-C \exp(-\lambda) \sum_{(k,l) \in \mathcal{P}_D^2} \left(\frac{1}{C_{\Xi, D} + 2(k+l)}\right)^2\right). \quad (33)$$

Since

$$\sum_{(k,l) \in \mathcal{P}_D^2} \left(\frac{1}{k+l}\right)^2 \geq |\mathcal{P}_D^2| \frac{1}{(2 \max \mathcal{P}_D)^2} \geq C, \quad (34)$$

the claim for $\gamma = 1$ now follows.

Step II.3: An upper bound for the case $\gamma < 1$

The same comparison as in the case $\gamma = 1$ can be made for $\gamma > 1$ yielding a suboptimal bound. Hence, for $\gamma < 1$ we need to proceed differently and assume that the stronger average Hölder condition (AHCb) holds. Partition the sets $B_{k,l}$ into $M_{k,l} \geq \frac{1}{8} \text{Leb}(B_{k,l})$ disjoint blocks $U_{k,l,j}$ of side-lengths one each, such that $\sup_{\mathbf{t} \in U_{k,l,j}} Z_{\mathbf{t}}$ and $\sup_{\mathbf{t} \in U_{k,l,j'}}$ $Z_{\mathbf{t}}$ are independent for $j \neq j'$ and discard the rest so that

$$\bigcup_{j=1}^{M_{k,l}} U_{k,l,j} \subset B_{k,l}, \quad \sum_{j=1}^{M_{k,l}} \text{Leb}(U_{k,l,j}) \geq \frac{1}{8} \text{Leb}(B_{k,l}).$$

$$\mathbb{P}\left(\max_{1 \leq j \leq M_{k,l}} \sup_{\mathbf{t} \in U_{k,l,j}} Z_{\mathbf{t}} \leq \Lambda_{k,l}\right) = \prod_{j=1}^{M_{k,l}} \mathbb{P}\left(\sup_{\mathbf{t} \in U_{k,l,j}} Z_{\mathbf{t}} \leq \Lambda_{k,l}\right).$$

By Theorem 7.1 in (Piterbarg, 1996) we deduce that

$$\begin{aligned} \prod_{(k,l) \in \mathcal{P}_D^2} \mathbb{P}\left(\sup_{\mathbf{t} \in B_{k,l}} \int \Xi(\mathbf{t} - \mathbf{z}) dW_{\mathbf{z}} \leq \Lambda_{k,l}\right) &\leq \prod_{(k,l) \in \mathcal{P}_D^2} \prod_{j=1}^{M_{k,l}} \mathbb{P}\left(\sup_{\mathbf{t} \in U_{k,l,j}} Z_{\mathbf{t}} \leq \Lambda_{k,l}\right) \\ &\leq \prod_{(k,l) \in \mathcal{P}_D^2} \prod_{j=1}^{M_{k,l}} \left(1 - C \Lambda_{k,l}^{\frac{d}{\gamma}-1} \exp\left(-\frac{1}{2} \Lambda_{k,l}^2\right)\right) \\ &= \exp\left(\sum_{(k,l) \in \mathcal{P}_D^2} \sum_{j=1}^{M_{k,l}} \log\left(1 - C \Lambda_{k,l}^{\frac{d}{\gamma}-1} \exp\left(-\frac{1}{2} \Lambda_{k,l}^2\right)\right)\right) \\ &\leq \exp\left(-\sum_{(k,l) \in \mathcal{P}_D^2} \sum_{j=1}^{M_{k,l}} C \Lambda_{k,l}^{\frac{d}{\gamma}-1} \exp\left(-\frac{1}{2} \Lambda_{k,l}^2\right)\right) \end{aligned}$$

We now plug in the definition of $\Lambda_{k,l}$ (see (31)) and obtain

$$\mathbb{P}(M_{\mathcal{B}_{k,l}} \leq \lambda) \leq \exp\left(-\exp(-\lambda - C\lambda^2/\log(n)) \left(1 + \frac{\lambda}{\log(n)}\right)^{\frac{d}{2\gamma}} \sum_{(k,l) \in \mathcal{P}_D^2} \frac{1}{\log\left(\frac{C_{\Xi}}{h_k h_l}\right)}\right).$$

The rest now follows as for (33), using (34).

Step III: Combination of the results

So far, we showed the result of the theorem for M_n only. In combination, the results from Step I and Step II show ensure that $M_n = O_{\mathbb{P}}(1)$. Hence, (28) and (32) become

$$\begin{aligned} &\max_{p,q \in \mathcal{P}_D^2} \max_{\mathbf{1}/h \in I_p \times I_q} \sup_{\mathbf{t} \in [1,1/h_p] \times [1,1/h_q]} \omega_{\mathbf{h}}(Z_{\mathbf{t}} - \omega_{\mathbf{h}}) \\ &\leq \max_{p,q \in \mathcal{P}_D^2} \sup_{\mathbf{t} \in [1,1/h_p] \times [1,1/h_q]} \omega_{(h_p, h_q)}(Z_{\mathbf{t}} - \omega_{(h_p, h_q)}) + O_{\mathbb{P}}\left(\frac{1}{\sqrt{\log(n)}}\right), \end{aligned}$$

respectively, and the claim of the theorem now follows. \square

6.1 Localization

Lemma 4. *If Assumption 1 c) is satisfied, the following holds true for a normed and uniformly bounded test-function $\Xi \in L^2[0, 1]^d$.*

$$\max_{i \in \{1, \dots, N\}} \left| \frac{1}{\sqrt{h_{i,1} \cdots h_{i,d}}} \int (\sigma(\mathbf{z}) - \sigma(\mathbf{t}_i)) \Xi \left(\frac{\mathbf{t}_i - \mathbf{z}}{\mathbf{h}_i} \right) dW_{\mathbf{z}} \right| = O_{\mathbb{P}}(\sqrt{\log(n)h_{\max}}) = o_{\mathbb{P}}(\log(n)^{-1/2}).$$

Proof of Lemma 4. Define

$$Y_{\mathbf{t}_i, \mathbf{h}_i}^{(1)} := \frac{1}{\sqrt{h_{i,1} \cdots h_{i,d}}} \int (\sigma(\mathbf{z}) - \sigma(\mathbf{t}_i)) \Xi \left(\frac{\mathbf{t}_i - \mathbf{z}}{\mathbf{h}_i} \right) dW_{\mathbf{z}},$$

$$Y_{\mathbf{t}_i, \mathbf{h}_i}^{(2)} := \frac{1}{\sqrt{h_{i,1} \cdots h_{i,d}}} \int \text{grad}(\sigma)(\mathbf{t}_i)(\mathbf{z} - \mathbf{t}_i) \Xi \left(\frac{\mathbf{t}_i - \mathbf{z}}{\mathbf{h}_i} \right) dW_{\mathbf{z}},$$

and, for $l = 1, 2$, $(i, j) \in \{1, \dots, N\}^2$, let $\gamma_{i,j}^{(l)} := \mathbb{E}[(Y_{\mathbf{t}_i, \mathbf{h}_i}^{(l)} - Y_{\mathbf{t}_j, \mathbf{h}_j}^{(l)})^2]$.

We have that

$$\sup_{(i,j) \in \{1, \dots, N\}^2} |\gamma_{i,j}^{(1)} - \gamma_{i,j}^{(2)}| \leq C(\|\Xi\|_2^2 + \|\Xi\|_{\infty}^2)h_{\max}. \quad (35)$$

Using Assumption (G) and (35), an application of Theorem 2.2.5 in (Adler and Taylor, 2007) yields

$$\left| \mathbb{E} \left[\max_{i \in \{1, \dots, N\}} Y_{\mathbf{t}_i, \mathbf{h}_i}^{(1)} \right] - \mathbb{E} \left[\max_{i \in \{1, \dots, N\}} Y_{\mathbf{t}_i, \mathbf{h}_i}^{(2)} \right] \right| \leq C\sqrt{h_{\max} \log(N)} = O(\sqrt{h_{\max} \log(n)}). \quad (36)$$

Define for $k \in \{1, \dots, d\}$ the quantities

$$\begin{aligned} Y_{\mathbf{t}_i, \mathbf{h}_i}^{(2,k)} &:= \frac{(\text{grad}(\sigma))_k(\mathbf{t}_i)}{\sqrt{h_{i,1} \cdots h_{i,d}}} \int (z_k - t_{i,k}) \Xi \left(\frac{\mathbf{t}_i - \mathbf{z}}{\mathbf{h}_i} \right) dW_{\mathbf{z}} \\ &= \frac{h_{i,k}(\text{grad}(\sigma))_k(\mathbf{t}_i)}{\sqrt{h_{i,1} \cdots h_{i,d}}} \int \frac{z_k - t_{i,k}}{h_{i,k}} \Xi \left(\frac{\mathbf{t}_i - \mathbf{z}}{\mathbf{h}_i} \right) dW_{\mathbf{z}} =: \frac{h_{i,k}(\text{grad}(\sigma))_k(\mathbf{t}_i)}{\sqrt{h_{i,1} \cdots h_{i,d}}} \int \tilde{\Xi}_k \left(\frac{\mathbf{t}_i - \mathbf{z}}{\mathbf{h}_i} \right) dW_{\mathbf{z}}, \end{aligned}$$

where $\tilde{\Xi}_k(\mathbf{z}) = z_k \Xi(\mathbf{z})$. By Theorem 3 we obtain that

$$\mathbb{E} \left[\max_{1 \leq i \leq N} \frac{1}{\sqrt{h_{i,1} \cdots h_{i,d}}} \int \tilde{\Xi} \left(\frac{\mathbf{t}_i - \mathbf{z}}{\mathbf{h}_i} \right) dW_{\mathbf{z}} \right] = O(\sqrt{\log(n)}).$$

Since $h_{i,k}(\text{grad}(\sigma))_k(\mathbf{t}_i) \leq Ch_{\max}$ we conclude that $\mathbb{E}[\max_{i \in \{1, \dots, N\}} Y_{\mathbf{t}_i, \mathbf{h}_i}^{(2)}] \leq C\sqrt{\log(n)h_{\max}}$ and hence, by (36), there exists a positive constant $C_{Y^{(1)}}$ such that $\mathbb{E}[\max_{i \in \{1, \dots, N\}} Y_{\mathbf{t}_i, \mathbf{h}_i}^{(1)}] \leq C_{Y^{(1)}}\sqrt{\log(n)h_{\max}}$. It follows by an application of Borell's inequality that, for $\lambda > C_{Y^{(1)}}$,

$$\mathbb{P} \left(\left| \max_{i \in \{1, \dots, N\}} Y_{\mathbf{t}_i, \mathbf{h}_i}^{(1)} \right| > \lambda \sqrt{\log(n)h_{\max}} \right) \leq \exp(-(\lambda - C_{Y^{(1)}})^2 \log(n)) = n^{-(\lambda - C_{Y^{(1)}})^2},$$

where we also used that $\max_{i \in \{1, \dots, N\}} \text{Var}(Y_{\mathbf{t}_i, \mathbf{h}_i}^{(1)}) \leq h_{\max}^2 \|\Xi\|_2^2 = h_{\max}^2$ since Ξ is normed. The assertion of the lemma now follows. \square

6.2 A continuous limit

Lemma 5. *Let Ξ be a test function satisfying Assumption 1 d) and let $\{\zeta_{\mathbf{k}} \mid \mathbf{k} \in \mathbb{N}^d\}$ be a field of independent, standard normally distributed random variables. Then*

$$\max_{1 \leq i \leq N} \left\{ (\sqrt{h_{i,1} \cdots h_{i,d}})^{-1} \left(n^{-\frac{d}{2}} \sum_{\mathbf{j} \in I_n} \zeta_{\mathbf{j}} \Xi \left(\frac{\mathbf{t}_i - \mathbf{x}_{\mathbf{j}}}{\mathbf{h}_i} \right) - \int \Xi \left(\frac{\mathbf{t}_i - \mathbf{x}_{\mathbf{j}}}{\mathbf{h}_i} \right) dW_{\mathbf{z}} \right) \right\} = o_{\mathbb{P}} \left(\frac{1}{\sqrt{\log(n)}} \right).$$

Proof of Lemma 5. Define the partial sum S_1 as follows:

$$S_1 = \sum_{1 \leq \mathbf{k} \leq 1} \zeta_{\mathbf{k}}, \quad \text{with } S_1 \equiv 0 \quad \text{if } \prod_{j=1}^d l_j = 0.$$

Each random variable $\zeta_{\mathbf{k}}$ can be expressed in terms of increments of the corresponding partial sum function,

$$\zeta_{\mathbf{k}} = \sum_{\alpha \in \{0,1\}^d} (-1)^{|\alpha|} S_{\mathbf{k}-\alpha}. \quad (37)$$

For each fixed $\mathbf{h} \in \mathcal{H}^2$, there exists a set $\mathcal{T}_{\mathbf{h}}$ such that $\max_{1 \leq i \leq N} F(\mathbf{t}_i, \mathbf{h}_i) = \max_{\mathbf{h} \in \mathcal{H}^2} \max_{\mathbf{t} \in \mathcal{T}_{\mathbf{h}}} F(\mathbf{t}, \mathbf{h})$. Let further $\frac{1}{\mathbf{h}}\mathcal{T}_{\mathbf{h}}$ denote the set $\{(t_1/h_1, t_2/h_2) \mid \mathbf{t} \in \mathcal{T}_{\mathbf{h}}\}$. For $\mathbf{t} \in \mathcal{T}_{\mathbf{h}}$ and $\mathbf{z}_{\mathbf{j}} := (j_1/(nh_1), \dots, j_d/(nh_d))$

$$\begin{aligned} & \sum_{1 \leq \mathbf{j} \leq \mathbf{n}-1} \int_{[\mathbf{z}_{\mathbf{j}}, \mathbf{z}_{\mathbf{j}+1})} \Xi(\mathbf{t} - \mathbf{z}_{\mathbf{j}}) dW_{\mathbf{z}} = \sum_{1 \leq \mathbf{j} \leq \mathbf{n}-1} \Xi\left(\frac{\mathbf{t}}{\mathbf{h}} - \mathbf{z}_{\mathbf{j}}\right) \sum_{\alpha \in \{0,1\}^d} (-1)^{|\alpha|} W(\mathbf{z}_{\mathbf{j}} - \alpha) \\ & \stackrel{\mathcal{D}}{=} (\sqrt{h_{i,1} \cdots h_{i,d}})^{-1} n^{-\frac{d}{2}} \sum_{1 \leq \mathbf{j} \leq \mathbf{n}-1} \Xi\left(\frac{\mathbf{t}}{\mathbf{h}} - \mathbf{z}_{\mathbf{j}}\right) \sum_{\alpha \in \{0,1\}^d} (-1)^{|\alpha|} W(\mathbf{j} - \alpha) \\ & \stackrel{\mathcal{D}}{=} (\sqrt{h_{i,1} \cdots h_{i,d}})^{-1} n^{-\frac{d}{2}} \sum_{1 \leq \mathbf{j} \leq \mathbf{n}-1} \Xi\left(\frac{\mathbf{t}}{\mathbf{h}} - \mathbf{z}_{\mathbf{j}}\right) \sum_{\alpha \in \{0,1\}^d} (-1)^{|\alpha|} S_{\mathbf{j}-\alpha} \\ & = (\sqrt{h_{i,1} \cdots h_{i,d}})^{-1} n^{-\frac{d}{2}} \sum_{1 \leq \mathbf{j} \leq \mathbf{n}-1} \Xi\left(\frac{\mathbf{t} - \mathbf{x}_{\mathbf{j}}}{\mathbf{h}}\right) \zeta_{\mathbf{j}}, \end{aligned}$$

where the last equality follows from (37). For fixed $\mathbf{h} \in \mathcal{H}^2$ and parameter $\mathbf{t} \in \frac{1}{\mathbf{h}}\mathcal{T}_{\mathbf{h}}$ consider the processes

$$Y_{\mathbf{t}}^{(1)} = Y_{\mathbf{t}}^{(1)}(\mathbf{h}) = \int \Xi(\mathbf{t} - \mathbf{z}) dW_{\mathbf{z}} - \sum_{1 \leq \mathbf{j} \leq \mathbf{n}-1} \int_{[\mathbf{z}_{\mathbf{j}}, \mathbf{z}_{\mathbf{j}+1})} \Xi(\mathbf{t} - \mathbf{z}) dW_{\mathbf{z}}$$

and

$$\begin{aligned} Y_{\mathbf{t}}^{(2)} &= Y_{\mathbf{t}}^{(2)}(\mathbf{h}) = \int \Xi(\mathbf{t} - \mathbf{z}) dW_{\mathbf{z}} - \int \Xi\left(\mathbf{t} - \left(\mathbf{z} + \frac{1}{n\mathbf{h}}\right)\right) dW_{\mathbf{z}} \\ &= \int \Xi(\mathbf{t} - \mathbf{z}) dW_{\mathbf{z}} - \int \sum_{1 \leq \mathbf{j} \leq \mathbf{n}-1} I_{[\mathbf{z}_{\mathbf{j}}, \mathbf{z}_{\mathbf{j}+1})}(\mathbf{z}) \Xi\left(\mathbf{t} - \left(\mathbf{z} + \frac{1}{n\mathbf{h}}\right)\right) dW_{\mathbf{z}}. \end{aligned}$$

We first show that

$$\mathbb{E} \left[\max_{\mathbf{t} \in \frac{1}{\mathbf{h}}\mathcal{T}_{\mathbf{h}}} Y_{\mathbf{t}}^{(2)} \right] = O\left(\frac{\sqrt{\log(n)}}{(nh_{\min})^\gamma}\right), \quad (38)$$

where γ is the degree of average smoothness (see (AHC)). By Assumption (AHC), for $\mathbf{t} \in \frac{1}{\mathbf{h}}\mathcal{T}_{\mathbf{h}}$, we immediately obtain

$$d_2(\mathbf{t}, \mathbf{t}') := \mathbb{E} \|Y_{\mathbf{t}}^{(2)} - Y_{\mathbf{t}'}^{(2)}\|^2 \leq C \|\mathbf{t} - \mathbf{t}'\|^{2\gamma}.$$

Hence, for all $\varepsilon > 0$ we find

$$\mathcal{N}(\varepsilon, \frac{1}{\mathbf{h}}\mathcal{T}_{\mathbf{h}}, d_2) \leq \frac{C}{h_{i,1} \cdots h_{i,d}} \left(\frac{1}{\varepsilon}\right)^{d/\gamma},$$

where $\mathcal{N}(\varepsilon, \frac{1}{\mathbf{h}}\mathcal{T}_{\mathbf{h}}, d_2)$ denotes the covering number of $\frac{1}{\mathbf{h}}\mathcal{T}_{\mathbf{h}}$ with respect to the (pseudo-)distance d_2 . Furthermore, also by Assumption (AHC), we find $\text{Var}[Y_{\mathbf{t}}^{(2)}] \leq L_{\Xi} \left(\frac{1}{nh_{\min}}\right)^{2\gamma}$. For $\lambda >$

$\sqrt{L_{\Xi}} \left(\frac{1}{nh_{\min}} \right)^{\gamma} (1 + \sqrt{d/\gamma})$, an application of Theorem 4.1.2 in (Adler and Taylor, 2007) yields

$$\mathbb{P} \left(\max_{\mathbf{t} \in \frac{1}{\mathbf{h}} \mathcal{T}_{\mathbf{h}}} Y_{\mathbf{t}}^{(2)} > \lambda \right) \leq \frac{C}{h_{i,1} \cdots h_{i,d}} \left(\frac{\lambda (nh_{\min})^{2\gamma}}{L_{\Xi} \sqrt{d/\gamma}} \right)^{d/\gamma} \bar{\psi} \left(\frac{\lambda (nh_{\min})^{\gamma}}{L_{\Xi}} \right), \quad (39)$$

where $\bar{\psi}(x) = \frac{1}{\sqrt{2\pi}} \int_x^{\infty} \exp(-\frac{1}{2}z^2) dz$ denotes the tail function of the standard normal distribution. We further obtain

$$\begin{aligned} \mathbb{E} \left[\max_{\mathbf{t} \in \frac{1}{\mathbf{h}} \mathcal{T}_{\mathbf{h}}} Y_{\mathbf{t}}^{(2)} \right] &\leq \mathbb{E} \left[\max_{\mathbf{t} \in \frac{1}{\mathbf{h}} \mathcal{T}_{\mathbf{h}}} |Y_{\mathbf{t}}^{(2)}| \right] = \int_0^{\infty} \mathbb{P} \left(\max_{\mathbf{t} \in \frac{1}{\mathbf{h}} \mathcal{T}_{\mathbf{h}}} |Y_{\mathbf{t}}^{(2)}| > \lambda \right) d\lambda \leq 2 \int_0^{\infty} \mathbb{P} \left(\max_{\mathbf{t} \in \frac{1}{\mathbf{h}} \mathcal{T}_{\mathbf{h}}} Y_{\mathbf{t}}^{(2)} > \lambda \right) d\lambda \\ &= 2 \int_0^{\frac{c\sqrt{\log(n)}}{(nh_{\min})^{\gamma}}} \mathbb{P} \left(\max_{\mathbf{t} \in \frac{1}{\mathbf{h}} \mathcal{T}_{\mathbf{h}}} Y_{\mathbf{t}}^{(2)} > \lambda \right) d\lambda + 2 \int_{\frac{c\sqrt{\log(n)}}{(nh_{\min})^{\gamma}}}^{\infty} \mathbb{P} \left(\max_{\mathbf{t} \in \frac{1}{\mathbf{h}} \mathcal{T}_{\mathbf{h}}} Y_{\mathbf{t}}^{(2)} > \lambda \right) d\lambda \\ &\leq \frac{2C\sqrt{\log(n)}}{(nh_{\min})^{\gamma}} + 2 \int_{\frac{c\sqrt{\log(n)}}{(nh_{\min})^{\gamma}}}^{\infty} \mathbb{P} \left(\max_{\mathbf{t} \in \frac{1}{\mathbf{h}} \mathcal{T}_{\mathbf{h}}} Y_{\mathbf{t}}^{(2)} > \lambda \right) d\lambda. \end{aligned}$$

Assertion (38) now follows from the tail bound (39), integration by parts and a proper adjustment of the constant C . We now show that for fixed $\mathbf{h} \in \mathcal{H}^2$, $Y_{\mathbf{t}}^{(1)}$ and $Y_{\mathbf{t}}^{(2)}$ are close to each other.

$$\left| \mathbb{E} \left[|Y_{\mathbf{t}}^{(1)} - Y_{\mathbf{t}'}^{(1)}|^2 \right] - \mathbb{E} \left[|Y_{\mathbf{t}}^{(2)} - Y_{\mathbf{t}'}^{(2)}|^2 \right] \right| \leq C \left(\left(\frac{1}{nh_{\min}} \right)^{2\gamma} + \left(\frac{1}{\log(n) \log \log(n)} \right)^2 \right). \quad (40)$$

An application of Theorem 2.2.5 in (Adler and Taylor, 2007) yields

$$\left| \mathbb{E} \left[\max_{\mathbf{t} \in \frac{1}{\mathbf{h}} \mathcal{T}_{\mathbf{h}}} Y_{\mathbf{t}}^{(1)} \right] - \mathbb{E} \left[\max_{\mathbf{t} \in \frac{1}{\mathbf{h}} \mathcal{T}_{\mathbf{h}}} Y_{\mathbf{t}}^{(2)} \right] \right| \leq C \sqrt{\log(N) \left(\left(\frac{1}{nh_{\min}} \right)^{2\gamma} + \frac{1}{\log(n)^2 \log \log(n)^2} \right)}.$$

Recall that, by Assumption (SR), we have $\gamma \in [1/2, 1]$ and $h_{\min} \geq \frac{C_{\min} \log(n)^3}{n \log \log(n)^2}$. Since, by Assumption (G), we also have $\log(N) = O(\log(n))$ and we obtain

$$\left| \mathbb{E} \left[\max_{\mathbf{t} \in \frac{1}{\mathbf{h}} \mathcal{T}_{\mathbf{h}}} Y_{\mathbf{t}}^{(1)} \right] - \mathbb{E} \left[\max_{\mathbf{t} \in \frac{1}{\mathbf{h}} \mathcal{T}_{\mathbf{h}}} Y_{\mathbf{t}}^{(2)} \right] \right| \leq C_{1,2} \frac{1}{\sqrt{\log(n) \log \log(n)}},$$

for some positive constant $C_{1,2}$. Let $\lambda > 2C_{1,2} + 1$. Then

$$\mathbb{P} \left(\left| \max_{\mathbf{t} \in \frac{1}{\mathbf{h}} \mathcal{T}_{\mathbf{h}}} Y_{\mathbf{t}}^{(1)} - \max_{\mathbf{t} \in \frac{1}{\mathbf{h}} \mathcal{T}_{\mathbf{h}}} Y_{\mathbf{t}}^{(2)} \right| > \frac{\lambda}{\sqrt{\log(n) \log \log(n)}} \right) \quad (41)$$

$$\leq \mathbb{P} \left(\left| \max_{\mathbf{t} \in \frac{1}{\mathbf{h}} \mathcal{T}_{\mathbf{h}}} Y_{\mathbf{t}}^{(1)} - \mathbb{E} \left[\max_{\mathbf{t} \in \frac{1}{\mathbf{h}} \mathcal{T}_{\mathbf{h}}} Y_{\mathbf{t}}^{(1)} \right] \right| > \frac{\lambda}{2\sqrt{\log(n) \log \log(n)}} \right) \quad (42)$$

$$+ \mathbb{P} \left(\left| \max_{\mathbf{t} \in \frac{1}{\mathbf{h}} \mathcal{T}_{\mathbf{h}}} Y_{\mathbf{t}}^{(2)} - \mathbb{E} \left[\max_{\mathbf{t} \in \frac{1}{\mathbf{h}} \mathcal{T}_{\mathbf{h}}} Y_{\mathbf{t}}^{(2)} \right] \right| > \frac{\lambda - 2C_{1,2}}{2\sqrt{\log(n) \log \log(n)}} \right). \quad (43)$$

For $j = 1, 2$, $\text{Var}(Y_{\mathbf{t}}^{(j)}) \leq 2L_{\Xi} (nh_{\min})^{-2\gamma} \leq 2L_{\Xi} \log \log(n)^2 / (\log(n)^3 C_{\min})$, an application of Borell's inequality to each of the two terms in (41) yields

$$\mathbb{P} \left(\left| \max_{\mathbf{t} \in \frac{1}{\mathbf{h}} \mathcal{T}_{\mathbf{h}}} Y_{\mathbf{t}}^{(1)} - \max_{\mathbf{t} \in \frac{1}{\mathbf{h}} \mathcal{T}_{\mathbf{h}}} Y_{\mathbf{t}}^{(2)} \right| > \frac{\lambda}{\sqrt{\log(n) \log \log(n)}} \right) \leq 4 \exp \left(- \frac{\log(n)^2 C_{\min}}{16L_{\Xi} \log \log(n)^4} \right) = o(n^{-\kappa}).$$

We can use the latter result to show that $Y_{\mathbf{t}}^{(1)}(\mathbf{h})$ and $Y_{\mathbf{t}}^{(2)}(\mathbf{h})$ are close to each other, uniformly

with respect to $\mathbf{h} \in \mathcal{H}^2$.

$$\begin{aligned} & \mathbb{P}\left(\left|\max_{\mathbf{h} \in \mathcal{H}^2} \max_{\mathbf{t} \in \frac{1}{h} \mathcal{T}_h} Y_{\mathbf{t}}^{(1)}(\mathbf{h}) - \max_{\mathbf{h} \in \mathcal{H}^2} \max_{\mathbf{t} \in \frac{1}{h} \mathcal{T}_h} Y_{\mathbf{t}}^{(2)}(\mathbf{h})\right| > \frac{\lambda}{\sqrt{\log(n)} \log \log(n)}\right) \\ & \leq \mathbb{P}\left(\left|\max_{\mathbf{h} \in \mathcal{H}^2} \max_{\mathbf{t} \in \frac{1}{h} \mathcal{T}_h} Y_{\mathbf{t}}^{(1)}(\mathbf{h}) - \max_{\mathbf{t} \in \frac{1}{h} \mathcal{T}_h} Y_{\mathbf{t}}^{(2)}(\mathbf{h})\right| > \frac{\lambda}{\sqrt{\log(n)} \log \log(n)}\right) \\ & \leq \sum_{\mathbf{h} \in \mathcal{H}^2} \mathbb{P}\left(\left|\max_{\mathbf{t} \in \frac{1}{h} \mathcal{T}_h} Y_{\mathbf{t}}^{(1)}(\mathbf{h}) - \max_{\mathbf{t} \in \frac{1}{h} \mathcal{T}_h} Y_{\mathbf{t}}^{(2)}(\mathbf{h})\right| > \frac{\lambda}{\sqrt{\log(n)} \log \log(n)}\right) = o(1) \quad \text{as } n \rightarrow \infty. \end{aligned}$$

In the same way, an application of Borell's inequality yields a tail bound for $\max_{\mathbf{t} \in \frac{1}{h} \mathcal{T}_h} Y_{\mathbf{t}}^{(2)}(\mathbf{h})$ which shows that $\max_{\mathbf{h} \in \mathcal{H}^2} \max_{\mathbf{t} \in \frac{1}{h} \mathcal{T}_h} Y_{\mathbf{t}}^{(2)}(\mathbf{h}) = O_{\mathbb{P}}((\log(n) \log \log(n))^{-\frac{1}{2}})$. The assertion of the Lemma now follows. \square

6.3 Gaussian Coupling

Lemma 6. *Suppose that Assumptions 1 and 2 hold. Then,*

$$\lim_{n \rightarrow \infty} \mathbb{P}_{H_0}(\mathcal{S}(Y) \leq q_{1-\alpha}^{S(W)}) \geq 1 - \alpha.$$

Proof of Lemma 6.

Step I: Gaussian coupling

Define

$$\Xi_i := \frac{\Phi_i}{n^{\frac{d}{2}} \|\sigma \Phi_i\|}, \quad X_{\mathbf{j}} := (\xi_{\mathbf{j}}(\sigma \Xi_i)(\mathbf{x}_{\mathbf{j}}))_{i=1}^N, \quad S_{i,n}(\xi) = \sum_{\mathbf{j} \in I_n} X_{\mathbf{j},i}, \quad \text{and } X := \max_{1 \leq i \leq N} S_{i,n}(\xi). \quad (44)$$

Consider a field of normally distributed random variables $\{\zeta_{\mathbf{j}} \sim \mathcal{N}(0, \sigma^2(\mathbf{x}_{\mathbf{j}})) \mid \mathbf{j} \in I_n\}$ and, as in (44), define the quantities $Z_{\mathbf{j}} := (\zeta_{\mathbf{j}} \sigma(\mathbf{x}_{\mathbf{j}}) \Xi_i(\mathbf{x}_{\mathbf{j}}))_{i=1}^N$ and $Z := \max_{1 \leq i \leq N} S_{i,n}(\zeta)$. By Corollary 4.1 in (Chernozhukov et al., 2014) it follows that

$$\mathbb{P}(|X - \tilde{Z}| > 16\Delta) \leq \frac{\{B_1 + \Delta^{-1}(B_2 + B_4)(d \vee \kappa) \log(n)\}(d \vee \kappa) \log(n)}{\Delta^2} + \frac{\Delta \log(n)}{n^d}, \quad (45)$$

for some $\tilde{Z} \stackrel{\mathcal{D}}{=} Z$ and all $\Delta > 0$, where B_1 , B_2 and B_4 are defined as follows:

$$B_1 = \mathbb{E}\left[\max_{1 \leq i, l \leq N} \left|\sum_{\mathbf{j} \in I_n} X_{\mathbf{j},i} X_{\mathbf{j},l} - \mathbb{E}[X_{\mathbf{j},i} X_{\mathbf{j},l}]\right|\right], \quad B_2 = \mathbb{E}\left[\max_{1 \leq i \leq N} \sum_{\mathbf{j} \in I_n} |X_{\mathbf{j},i}|^3\right]$$

and

$$B_4 = \sum_{\mathbf{j} \in I_n} \mathbb{E}\left[\max_{1 \leq i \leq N} |X_{\mathbf{j},i}|^3 \mathbf{1}\left\{\max_{1 \leq i \leq N} |X_{\mathbf{j},i}| \geq \frac{\Delta}{(d \vee \kappa) \log(n)}\right\}\right].$$

Define

$$U_{\mathbf{j};i,l} := X_{\mathbf{j},i} X_{\mathbf{j},l} - \mathbb{E}[X_{\mathbf{j},i} X_{\mathbf{j},l}] = (\xi_{\mathbf{j}}^2 - \sigma^2(\mathbf{x}_{\mathbf{j}})) \frac{\Phi_l(\mathbf{x}_{\mathbf{j}}) \Phi_i(\mathbf{x}_{\mathbf{j}})}{n^d \|\sigma \Phi_l\| \|\sigma \Phi_i\|},$$

$$B_{i,l} := \frac{\max_{\mathbf{j} \in I_n} |\Phi_l(\mathbf{x}_{\mathbf{j}}) \Phi_i(\mathbf{x}_{\mathbf{j}})|}{n^d \|\sigma \Phi_i\| \|\sigma \Phi_l\|} \leq \frac{\|\Phi\|_{\infty}^2}{c_{\sigma}^2 (nh_{\min})^d} \quad \text{and} \quad v_{\mathbf{j};i,l} := M \frac{\Phi_l^2(\mathbf{x}_{\mathbf{j}}) \Phi_i^2(\mathbf{x}_{\mathbf{j}})}{n^{2d} \|\sigma \Phi_i\|^2 \|\sigma \Phi_l\|^2}.$$

By the structure of the dictionary (5) and boundedness of Φ by Assumption 1 d), we immediately obtain $B_{i,l} \leq \frac{\|\Phi\|_{\infty}^2}{c_{\sigma}^2 (nh_{\min})^d}$, where $c_{\sigma}^2 > 0$ is a uniform lower bound on σ^2 which exists by Assumption

(M2). By the moment condition (M1) we obtain $\mathbb{E}|U_{j;i,l}|^J \leq \frac{1}{2}J! v_{j;i,l} \cdot B_{i,l}^{J-2}$, $J \geq 2$. Hence, we can bound B_1 using the Bernstein inequality (cf. (van der Vaart and Wellner, 1996), Lemma 2.2.11) as follows. Using $\sum_{j \in I_n} v_{j;l,i} \leq 2 \frac{\|\Phi\|_\infty^4}{c_\sigma^4 (nh_{\min})^d}$ and

$$\mathbb{P}\left(\left|\sum_{j \in I_n} U_{j;l,i}\right| > x\right) \leq 2 \exp\left(-\frac{x^2}{2 \sum_{j \in I_n} v_{j;l,i} + 2xB_{i,l}}\right) \leq 2 \exp\left(-\frac{x^2 (nh_{\min})^d}{4c_\sigma^{-4} \|\Phi\|_\infty^4 + 2x4c_\sigma^{-2} \|\Phi\|_\infty^2}\right), \quad (46)$$

we find, for an arbitrary constant \mathcal{C} ,

$$\begin{aligned} B_1 &\leq \mathcal{C} \sqrt{\log(n)} \left(\sum_{j \in I_n} v_{j;i,l}\right)^{\frac{1}{2}} + N^2 \max_{i,l} \mathbb{E} \left[\left| \sum_{j \in I_n} U_{j;l,i} \mathbb{1} \left\{ \left| \sum_{j \in I_n} U_{j;l,i} \right| > \mathcal{C} \sqrt{\log(n)} \left(\sum_{j \in I_n} v_{j;i,l}\right)^{\frac{1}{2}} \right\} \right| \right] \\ &\leq O\left(\left(\frac{1}{nh_{\min}}\right)^{\frac{d}{2}} \sqrt{\log(n)}\right) + N^2 \max_{i,l} \int_{\mathcal{C} \sqrt{\log(n)} \left(\sum_{j \in I_n} v_{j;i,l}\right)^{\frac{1}{2}}}^{\infty} \mathbb{P}\left(\left|\sum_{j \in I_n} U_{j;l,i}\right| > x\right) dx \\ &\quad + N^2 \mathcal{C} \max_{i,l} \sqrt{\log(n)} \left(\sum_{j \in I_n} v_{j;i,l}\right)^{\frac{1}{2}} \mathbb{P}\left(\left|\sum_{j \in I_n} U_{j;l,i}\right| > \mathcal{C} \sqrt{\log(n)} \left(\sum_{j \in I_n} v_{j;i,l}\right)^{\frac{1}{2}}\right). \end{aligned}$$

For a sufficiently large choice of the constant \mathcal{C} , by (46) we find

$$B_1 = O\left(\left(\frac{1}{nh_{\min}}\right)^{\frac{d}{2}} \sqrt{\log(n)}\right). \quad (47)$$

Recall that by assumption, the support of Φ is contained in $[0, 1]^d$ and Φ is uniformly bounded. Then, the moment assumptions (M1) and (M2) imply

$$B_2 = \mathbb{E} \left[\max_{1 \leq i \leq N} \sum_{j \in n[\mathbf{t}_i - \mathbf{h}_i, \mathbf{t}_i]} |X_{j,i}|^3 \right] \leq \frac{C}{(nh_{\min})^{\frac{d}{2}}}. \quad (48)$$

For the estimation of the term B_4 we make use of the moment assumption (M1) once more and find

$$\mathbb{E}[\exp(\theta|\xi_j^2 - \sigma^2(\mathbf{x}_j)|)] \leq \exp\left(\theta \mathbb{E}|\xi_j^2 - \sigma^2(\mathbf{x}_j)| + \frac{\theta^2 \mathbb{E}|\xi_j^2 - \sigma^2(\mathbf{x}_j)|^2}{2(1-\theta)}\right) \quad \text{for } \theta \in [0, 1].$$

Hence, for $\theta = 0.5$,

$$\mathbb{E}[\exp(\theta|\xi_j^2 - \sigma^2(\mathbf{x}_j)|)] \leq e^{\frac{3}{4}M}, \quad (49)$$

where the constant M is a uniform upper bound on the fourth moments of the ξ_j which exists due to (M2). We further obtain

$$\begin{aligned} B_4 &\leq \frac{C}{(nh_{\min})^{\frac{3d}{2}}} \left(\sum_{j \in I_n} \mathbb{E} \left[\mathbb{1} \left\{ |\xi_j^2 - \sigma^2(\mathbf{x}_j)| + \sigma^2(\mathbf{x}_j) > \left(\frac{\Delta(nh_{\min})^{d/2}}{4\kappa \log(n)}\right)^2 \right\} \right] \right)^{\frac{1}{2}} \\ &\leq \frac{Cn^d}{(nh_{\min})^{\frac{3d}{2}}} \left(\exp\left(-\frac{c_\sigma^2}{16} (nh_{\min})^2 \Delta^2 / \log(n)^2\right) \right)^{\frac{1}{2}}. \end{aligned}$$

Step II: The level is maintained

Define

$$P_{0,n} := \mathbb{P}_{H_0} \left(\mathcal{S}(Y) \leq q_{1-\alpha}^{\mathcal{S}(W)} \right) = \mathbb{P}_{H_0} \left(\langle Y, \Phi_i \rangle_n \leq q_{i,1-\alpha} \quad \forall 1 \leq i \leq N \right)$$

We now show that $\lim_{n \rightarrow \infty} P_{0,n} \geq 1 - \alpha$.

We have that

$$\begin{aligned}
P_{0,n} &= \mathbb{P}_{H_0} \left(\langle Y, \Phi_i \rangle_n \leq \sigma_i \left(\frac{q_{1-\alpha}^{S(W)}}{\omega_i} + \omega_i \right) \forall 1 \leq i \leq N \right) \\
&\geq \mathbb{P}_{H_0} \left(\langle Y, \Phi_i \rangle_n \leq \left(\frac{q_{1-\alpha}^{S(W)}}{\omega_i} + \omega_i \right) (1 - |r_n|) \forall 1 \leq i \leq N \right) \\
&= \mathbb{P}_{H_0} \left(\frac{1}{n^{\frac{d}{2}} \|\Phi\| \sqrt{h_{i,1} h_{i,2}}} \sum_{\mathbf{j} \in I_n} \xi_{\mathbf{j}} \Phi_i(\mathbf{x}_{\mathbf{j}}) \leq \left(\frac{q_{1-\alpha}^{S(W)}}{\omega_i} + \omega_i \right) (1 - |r_n|) \forall 1 \leq i \leq N \right),
\end{aligned}$$

for $r_n = o(1/\log(n))$, since $n^d \|\Phi_i \sigma\|_2^2 = \text{Var}(\langle Y, \Phi_i \rangle_n) + o(1/\log(n))$, uniformly in i .

Step II.1: Reduction of the set of scales

We now separate the variables \mathbf{t}_i and \mathbf{h}_i and proceed as in Step I.1 in the proof of Theorem 3 .

Recall that $h_{p,D} = h_p = \exp(-D(p+1))$ denotes the smallest scale in each slice and that for any fixed $\mathbf{h} \in \mathcal{H}_D^2 = \{h_p | p \in \mathcal{P}_D\}$, there exists a set $\mathcal{T}_{\mathbf{h}}$ such that $\max_{1 \leq i \leq N} F(\mathbf{t}_i, \mathbf{h}_i) = \max_{\mathbf{h} \in \mathcal{H}_D^2} \max_{\mathbf{t} \in \mathcal{T}_{\mathbf{h}}} F(\mathbf{t}, \mathbf{h})$. With the same arguments as in the proof of Theorem 3, we only consider scales $\mathbf{h} \in \mathcal{H}_D^2$. By construction, we have that $|\mathcal{H}_D| = O(\log(n))$. This yields

$$\begin{aligned}
P_{0,n} &\geq \mathbb{P}_{H_0} \left(\frac{1}{n^{\frac{d}{2}} \|\Phi\| \sqrt{h_1 h_2}} \sum_{\mathbf{j} \in I_n} \xi_{\mathbf{j}} \Phi \left(\frac{\mathbf{t} - \mathbf{x}_{\mathbf{j}}}{\mathbf{h}} \right) \leq \left(\frac{q_{1-\alpha}^{S(W)}}{\omega_{\mathbf{h}}} + \omega_{\mathbf{h}} \right) (1 - |r_n|) \forall (\mathbf{t}, \mathbf{h}) \in \mathcal{T}_{\mathbf{h}} \times \mathcal{H}_D^2 \right) \\
&= \mathbb{P}_{H_0} \left(\frac{1}{n^{\frac{d}{2}} \|\Phi\| \sqrt{h_p h_q}} \sum_{\mathbf{j} \in I_n} \xi_{\mathbf{j}} \Phi \left(\frac{\mathbf{t} - \mathbf{x}_{\mathbf{j}}}{\mathbf{h}_{p,q}} \right) \leq \left(\frac{q_{1-\alpha}^{S(W)}}{\omega_{\mathbf{h}_{p,q}}} + \omega_{\mathbf{h}_{p,q}} \right) (1 - |r_n|) \forall (\mathbf{t}, p, q) \in \mathcal{T}_{\mathbf{h}} \times \mathcal{P}_D^2 \right),
\end{aligned}$$

where $\mathbf{h}_{p,q} = (h_p, h_q)$. Let further $\frac{1}{\mathbf{h}} \mathcal{T}_{\mathbf{h}}$ denote the set $\{(t_1/h_1, t_2/h_2) | \mathbf{t} \in \mathcal{T}_{\mathbf{h}}\}$. Then

$$P_{0,n} \geq \mathbb{P}_{H_0} \left(\frac{1}{n^{\frac{d}{2}} \|\Phi\| \sqrt{h_p h_q}} \sum_{\mathbf{j} \in I_n} \xi_{\mathbf{j}} \Phi \left(\mathbf{t} - \frac{\mathbf{x}_{\mathbf{j}}}{\mathbf{h}_{p,q}} \right) \leq \left(\frac{q_{1-\alpha}^{S(W)}}{\omega_{\mathbf{h}_{p,q}}} + \omega_{\mathbf{h}_{p,q}} \right) (1 - |r_n|) \forall (\mathbf{t}, p, q) \in \frac{1}{\mathbf{h}} \mathcal{T}_{\mathbf{h}} \times \mathcal{P}_D^2 \right),$$

where $\frac{\mathbf{x}_{\mathbf{j}}}{\mathbf{h}_{p,q}}$ denotes component-wise division. Replace each set

$$\frac{1}{\mathbf{h}} \mathcal{T}_{\mathbf{h}} \quad \text{by} \quad \frac{1}{\tilde{\mathbf{h}}} \tilde{\mathcal{T}}_{\tilde{\mathbf{h}}} := \bigcup_{\tilde{\mathbf{h}} \leq \mathbf{h}} \frac{1}{\tilde{\mathbf{h}}} \mathcal{T}_{\tilde{\mathbf{h}}},$$

where the inequality $\tilde{\mathbf{h}} \leq \mathbf{h}$ is meant component-wise. It follows that

$$P_{0,n} \geq \mathbb{P}_{H_0} \left(\frac{1}{n^{\frac{d}{2}} \|\Phi\| \sqrt{h_p h_q}} \sum_{\mathbf{j} \in I_n} \xi_{\mathbf{j}} \Phi \left(\mathbf{t} - \frac{\mathbf{x}_{\mathbf{j}}}{\mathbf{h}_{p,q}} \right) \leq \left(\frac{q_{1-\alpha}^{S(W)}}{\omega_{\mathbf{h}_{p,q}}} + \omega_{\mathbf{h}_{p,q}} \right) (1 - |r_n|) \forall (\mathbf{t}, p, q) \in \frac{1}{\tilde{\mathbf{h}}} \tilde{\mathcal{T}}_{\tilde{\mathbf{h}}} \times \mathcal{P}_D^2 \right),$$

and the total number of (\mathbf{t}, \mathbf{h}) considered is still of polynomial order in n .

Step II.2: Partition of the parameter set

We partition the parameter set for \mathbf{t} in the same way as in step I.2 of the proof of Theorem 3. The blocks $B_{k,l}$ are constructed such that the suprema over different blocks are independent since $\text{supp} \Phi \subset [0, 1]^d$. This yields

$$\mathbf{q}_{k,l} := \left(\frac{q_{1-\alpha}^{S(W)}}{\omega_{\mathbf{h}_{k,l}}} + \omega_{\mathbf{h}_{k,l}} \right) = \min_{(k,l) \leq (i,j)} \left(\frac{q_{1-\alpha}^{S(W)}}{\omega_{\mathbf{h}_{i,j}}} + \omega_{\mathbf{h}_{i,j}} \right).$$

$$\begin{aligned}
P_{0,n} &\geq \prod_{(k,l) \in \mathcal{P}_D^2} \mathbb{P} \left(\max_{(k,l) \leq (p,q)} \max_{\mathbf{t} \in B_{k,l} \cap \frac{1}{\tilde{\mathbf{h}}} \tilde{\mathcal{T}}_{\tilde{\mathbf{h}}}} \frac{1}{n^{\frac{d}{2}} \|\Phi\| \sqrt{h_p h_q}} \sum_{\mathbf{j} \in I_n} \xi_{\mathbf{j}} \Phi \left(\mathbf{t} - \frac{\mathbf{x}_{\mathbf{j}}}{\mathbf{h}_{p,q}} \right) \leq \mathbf{q}_{k,l} (1 - |r_n|) \right) \\
&\geq \prod_{(k,l) \in \mathcal{P}_D^2} \mathbb{P} \left(\max_{\mathbf{t} \in B_{k,l} \cap \frac{1}{\tilde{\mathbf{h}}} \tilde{\mathcal{T}}_{\tilde{\mathbf{h}}}} \max_{(p,q) \in \mathcal{P}_D^2} \frac{1}{n^{\frac{d}{2}} \|\Phi\| \sqrt{h_p h_q}} \sum_{\mathbf{j} \in I_n} \xi_{\mathbf{j}} \Phi \left(\mathbf{t} - \frac{\mathbf{x}_{\mathbf{j}}}{\mathbf{h}_{p,q}} \right) \leq \mathbf{q}_{k,l} (1 - |r_n|) \right).
\end{aligned}$$

By the results of Step I, for each fixed pair (k, l) , we can now replace the variables $\xi_{\mathbf{j}}$ by Gaussian ones. Each set of Gaussian random variables depends on k and l , but the corresponding distributions do not. By (45), it follows that

$$P_{0,n} \geq \prod_{(k,l) \in \mathcal{P}_D^2} \left\{ \mathbb{P} \left(\max_{\mathbf{t} \in B_{k,l} \cap \frac{1}{h} \tilde{\mathcal{T}}_h} \max_{(p,q) \in \mathcal{P}_D^2} \frac{1}{n^{\frac{d}{2}} \|\Phi\| \sqrt{h_p h_q}} \sum_{\mathbf{j} \in I_n} \zeta_{\mathbf{j}} \Phi \left(\mathbf{t} - \frac{\mathbf{x}_{\mathbf{j}}}{\mathbf{h}_{p,q}} \right) > \mathbf{q}_{k,l} (1 - |r_n|) - \Delta_n \right) \right. \\ \left. \times \left(1 - C |\mathcal{P}_D|^2 \Delta_n^{-2} \{B_1 + \Delta_n^{-1} (B_2 + B_4) \log(n)\} \log(n) + \frac{|\mathcal{P}_D|^2 \Delta_n \log(n)}{n^d} \right) \right\}.$$

By assumption, $h_{\min} \gtrsim n^{-1} \log(n)^{\frac{15}{d} \vee 3} \log \log(n)^2$. Hence, choosing $\Delta_n = 1/(\sqrt{\log(n) \log \log(n)})$, the results from Step I give, uniformly in k and l

$$|\mathcal{P}_D|^2 \Delta_n^{-2} \{B_1 + \Delta_n^{-1} (B_2 + B_4) \log(n)\} \log(n) + \frac{|\mathcal{P}_D|^2 \Delta_n \log(n)}{n^d} = O \left(\frac{1}{\log(n)^2 \sqrt{\log(\log(n))}} \right).$$

This yields

$$P_{0,n} \geq \left\{ \prod_{(k,l) \in \mathcal{P}_D^2} \mathbb{P} \left(\max_{\mathbf{t} \in B_{k,l} \cap \frac{1}{h} \tilde{\mathcal{T}}_h} \max_{(p,q) \in \mathcal{P}_D^2} \frac{1}{n^{\frac{d}{2}} \|\Phi\| \sqrt{h_p h_q}} \sum_{\mathbf{j} \in I_n} \zeta_{\mathbf{j}} \Phi \left(\mathbf{t} - \frac{\mathbf{x}_{\mathbf{j}}}{\mathbf{h}_{p,q}} \right) \leq \mathbf{q}_{k,l} (1 - |r_n|) - \Delta_n \right) \right\} \\ \times \left(1 - \frac{1}{\sqrt{\log \log(n)} |\mathcal{P}_D|^2} \right)^{|\mathcal{P}_D|^2}.$$

Using Lemma 5, we replace the sum by the corresponding Wiener integral

$$P_{0,n} \geq (1 - o(1)) \prod_{(k,l) \in \mathcal{P}_D^2} \mathbb{P} \left(\max_{\mathbf{t} \in B_{k,l}} \int \Xi(\mathbf{t} - \mathbf{z}) dW_{\mathbf{z}} \leq \mathbf{q}_{k,l} (1 - |r_n|) - o(1/\sqrt{\log(n)}) \right),$$

where $\Xi = \Phi/\|\Phi\|$. Finally,

$$P_{0,n} \geq (1 - o(1)) \mathbb{P} \left(\max_{(k,l) \in \mathcal{P}_D^2} \omega_{k,l} \left(\max_{\mathbf{t} \in B_{k,l}} \int \Xi(\mathbf{t} - \mathbf{z}) dW_{\mathbf{z}} - \omega_{k,l} \right) \leq q_{1-\alpha}^{\mathcal{S}(W)} - o(1) \right) \\ \geq (1 - o(1)) \mathbb{P} \left(\max_{(k,l) \in \mathcal{P}_D^2} \omega_{k,l} \left(\max_{\mathbf{t} \in [1, 1/h_{k,l}]} \int \Xi(\mathbf{t} - \mathbf{z}) dW_{\mathbf{z}} - \omega_{k,l} \right) \leq q_{1-\alpha}^{\mathcal{S}(W)} - o(1) \right),$$

which implies $\lim_{n \rightarrow \infty} P_{0,n} \geq 1 - \alpha$. \square

6.4 Unbounded Support

Theorem 4. *If Ξ is of unbounded support but decays sufficiently fast, i. e.,*

$$\int (1 + \|\mathbf{z}\|^2)^{\frac{1}{2}} \Xi^2(\mathbf{z}) d\mathbf{z} < \infty, \quad (\text{Decay})$$

the results of Theorem 3 still hold.

Proof of Theorem 4. Let χ_n be a sequence of smooth functions with $\text{supp} \chi_n = [-\log(n)^3, \log(n)^3]^d$. Define

$$\tilde{\Xi} := \chi_n \cdot \Xi \quad \text{and} \quad \Xi_{\Delta} := \Xi - \tilde{\Xi}$$

and the corresponding process

$$Z_{\Delta, \mathbf{t}} := \int \Xi_{\Delta}(\mathbf{t} - \mathbf{z}) dW_{\mathbf{z}}.$$

Using (Decay), we obtain

$$\text{Var}(Z_{\Delta, \mathbf{t}}) \leq \sum_{j=1}^d \int_{\{|t_j - z_j| > \log(n)^3\}} \Xi_{\Delta}(\mathbf{t} - \mathbf{z})^2 d\mathbf{z} \leq \frac{C}{\log(n)^3}.$$

With the same arguments as for (39) in the proof of Lemma 5 we obtain

$$\mathbb{P}\left(\sup_{\mathbf{t} \in [1, 1/\mathbf{h}]} Z_{\Delta, \mathbf{t}} > \lambda/(\log(n)^2 \log(\log(n)))\right) \leq Cn^{-\lambda}.$$

Hence, $Z_{\Delta, \mathbf{t}}$ is asymptotically negligible. For the term $Z_{\Delta, \mathbf{t}}$ the same arguments as in the proof of Theorem 3 apply. We use the same slicing technique as in Step I.1. Then we partition the parameter set in the same way as in Step I.2 of the proof of Theorem 3 separating the main blocks by stripes of widths and lengths $2 \log(n)^3$. Since $|1/h_i - 1/h_{i+1}| \geq C/h_{\max} \gtrsim n^\delta$, those are still small in comparison. A careful inspection of the proof of Theorem 3 shows that the same arguments apply in this case as well. \square

6.5 Proofs of the main results

Proof of Theorem 1. The proof of this theorem is a combination of the subsequent applications of the auxiliary results of the previous subsection. The Gaussian approximation follows from Lemma 6. The continuous approximation is valid due to Lemma 5. An application of Lemma 4 yields a distribution free approximation to which, finally, Theorem 3 is applied for $\Xi = \Phi/\|\Phi\|_2$. \square

Proof of Theorem 2. Let

$$\delta_{\mathbf{t}, \mathbf{h}} := \frac{1}{\sqrt{h_{i,1} \cdots h_{i,d}}} \int \Xi\left(\frac{\mathbf{t} - \mathbf{z}}{\mathbf{h}}\right) dW_{\mathbf{z}} - \frac{1}{\sqrt{h_{i,1} \cdots h_{i,d}}} \int (\Xi \cdot \mathbb{1}_{[-\rho, 1+\rho]^d})\left(\frac{\mathbf{t} - \mathbf{z}}{\mathbf{h}}\right) dW_{\mathbf{z}}.$$

Using (Decay) and by a change of variables, we obtain

$$\text{Var}(\Delta_{\mathbf{t}, \mathbf{h}}) \leq \sum_{j=1}^d \int_{\{|x_j| > \rho/h_j\}} \Xi_{\Delta}(\mathbf{x})^2 d\mathbf{x} \leq \frac{C}{\log(n)^\tau},$$

for some $\tau > 0$. With the same arguments as for (39) in the proof of Lemma 5 we obtain

$$\mathbb{P}\left(\sup_{\mathbf{t} \in [\mathbf{h}, \mathbf{1}]} \Delta_{\mathbf{t}, \mathbf{h}} > \lambda/(\log(n)^2 \log(\log(n)))\right) \leq Cn^{-\lambda}.$$

The claim of the Theorem now follows by an application of Theorem 4. \square

Proof of Lemma 1. We have that

$$\begin{aligned} & \mathbb{P}(\langle Y, \Phi_i \rangle_n > q_{i, 1-\alpha} \quad \forall i \in \mathcal{I}_{2, \alpha}) \\ &= \mathbb{P}(\langle \xi, \Phi_i \rangle_n + \langle f, \varphi_i \rangle + o(1/\log(n)^2) > q_{i, 1-\alpha} \quad \forall i \in \mathcal{I}_{2, \alpha}) \\ &\geq \mathbb{P}(\langle \xi, \Phi_i \rangle_n + o(1/\log(n)^2) > -q_{i, 1-\alpha} \quad \forall i \in \mathcal{I}_{2, \alpha}) \end{aligned}$$

Thus, the claim of the lemma now follows by an application of Theorem 1 and by the same arguments if $k = 1$. \square

Finally, the claims of Lemmas 2 and 3 follow by the same arguments as Lemma 1, which concludes this section.

Acknowledgements

The authors gratefully acknowledge financial support by the German Research Foundation DFG through subproject A07 of CRC 755. Funding through the VW foundation is also gratefully acknowledged. Furthermore we thank Haisen Ta and Jan Keller who are with the lab of Stefan Hell at the Department of NanoBiophotonics, Max Planck Institute for Biophysical Chemistry for providing the experimental data and expertise.

References

- Abramovich, F. and Silverman, B. W. (1998). Wavelet decomposition approaches to statistical inverse problems. *Biometrika*, 85:115–129.
- Adler, R. J. and Taylor, J. E. (2007). *Random Fields and Geometry*. Springer, New York.
- Albani, V., Elbau, P., de Hoop, M. V., and Scherzer, O. (2016). Optimal convergence rates results for linear inverse problems in Hilbert spaces. *Numer. Funct. Anal. Optim.*, 37(5):521–540.
- Anderssen, R. S. (1986). The linear functional strategy for improperly posed problems. In *Inverse Problems*, pages 11–30. Springer.
- Arias-Castro, E., Donoho, D. L., and Huo, X. (2005). Near-optimal detection of geometric objects by fast multiscale methods. *IEEE Trans. Inform. Theory*, 51(7):2402–2425.
- Aspelmeier, T., Egner, A., and Munk, A. (2015). Modern statistical challenges in high-resolution fluorescence microscopy. *Annu. Rev. Stat. Appl.*, 2:163–202.
- Bertero, M., Boccacci, P., Desiderà, G., and Vicidomini, G. (2009). Image deblurring with Poisson data: from cells to galaxies. *Inverse Probl.*, 25(12):025004, 18.
- Bissantz, N., Claeskens, G., Holzmann, H., and Munk, A. (2009). Testing for lack of fit in inverse regression—with applications to biophotonic imaging. *J. R. Stat. Soc. Ser. B Stat. Methodol.*, 71(1):25–48.
- Bissantz, N., Hohage, T., Munk, A., and Ruymgaart, F. (2007). Convergence rates of general regularization methods for statistical inverse problems and applications. *SIAM J. Numer. Anal.*, 45(6):2610–2636.
- Born, M. and Wolf, E. (1999). *Principles of Optics*. Cambridge University Press, Cambridge, seventh edition.
- Burger, M., Flemming, J., and Hofmann, B. (2013). Convergence rates in regularization if the sparsity assumption fails. *Inverse Probl.*, 29(2):025013.
- Butucea, C. (2007). Goodness-of-fit testing and quadratic functional estimation from indirect observations. *Ann. Statist.*, 35(5):1907–1930.
- Butucea, C. and Comte, F. (2009). Adaptive estimation of linear functionals in the convolution model and applications. *Bernoulli*, 15(1):69–98.
- Cai, T. and Yuan, M. (2014). Rate-optimal detection of very short signal segments. arXiv:1407.2812.
- Cai, T. T., Jeng, X. J., and Li, H. (2012). Robust detection and identification of sparse segments in ultrahigh dimensional data analysis. *J. R. Stat. Soc. Ser. B. Stat. Methodol.*, 74(5):773–797.
- Cavalier, L. (2011). Inverse problems in statistics. In *Inverse problems and high-dimensional estimation*, volume 203 of *Lect. Notes Stat. Proc.*, pages 3–96. Springer, Heidelberg.

- Cavalier, L. and Golubev, Y. (2006). Risk hull method and regularization by projections of ill-posed inverse problems. *Ann. Statist.*, 34(4):1653–1677.
- Cavalier, L., Golubev, Y., Lepski, O., and Tsybakov, A. (2003). Block thresholding and sharp adaptive estimation in severely ill-posed inverse problems. *Teor. Veroyatnost. i Primenen.*, 48(3):534–556.
- Cavalier, L. and Tsybakov, A. (2002). Sharp adaptation for inverse problems with random noise. *Probab. Theory Related Fields*, 123(3):323–354.
- Chernousova, E. and Golubev, Y. (2014). Spectral cut-off regularizations for ill-posed linear models. *Math. Methods Statist.*, 23(2):116–131.
- Chernozhukov, V., Chetverikov, D., and Kato, K. (2014). Gaussian approximation of suprema of empirical processes. *Ann. Statist.*, 42:1564–1597.
- Cohen, A., Hoffmann, M., and Reiß, M. (2004). Adaptive wavelet Galerkin methods for linear inverse problems. *SIAM J. Numer. Anal.*, 42(4):1479–1501.
- Dedecker, J., Merlevède, F., and Rio, E. (2014). Strong approximation of the empirical distribution function for absolutely regular sequences in \mathbb{R}^d . *Electron. J. Probab.*, 19(9):1–56.
- Donoho, D. and Jin, J. (2004). Higher criticism for detecting sparse heterogeneous mixtures. *Ann. Statist.*, pages 962–994.
- Donoho, D. L. (1995). Nonlinear solution of linear inverse problems by wavelet-vaguelette decomposition. *Appl. Comput. Harmon. Anal.*, 2(2):101–126.
- Dümbgen, L. and Spokoiny, V. (2001). Multiscale testing of qualitative hypotheses. *The Annals of Statistics*, 29(1):124–152.
- Dümbgen, L. and Walther, G. (2008). Multiscale inference about a density. *Ann. Statist.*, 36(4):1758–1785.
- Frick, K., Munk, A., and Sieling, H. (2014). Multiscale change point inference. *J. R. Stat. Soc. Ser. B. Stat. Methodol.*, 76(3):495–580. With 32 discussions by 47 authors and a rejoinder by the authors.
- Friedenberg, D. A. and Genovese, C. R. (2013). Straight to the source: detecting aggregate objects in astronomical images with proper error control. *J. Amer. Statist. Assoc.*, 108(502):456–468.
- Genovese, C. R., Perone-Pacifco, M., Verdinelli, I., and Wasserman, L. (2012). The geometry of nonparametric filament estimation. *J. Amer. Statist. Assoc.*, 107(498):788–799.
- Glaz, J., Naus, J., and Wallenstein, S. (2001). *Scan Statistics*. Springer Series in Statistics. Springer-Verlag, New York.
- Goldenshluger, A. (1999). On pointwise adaptive nonparametric deconvolution. *Bernoulli*, 5(5):907–925.
- Hell, S. (2007). Far-field optical nanoscopy. *Science*, 316:1153 – 1158.
- Hell, S. W. and Wichmann, J. (1994). Breaking the diffraction resolution limit by stimulated emission: stimulated-emission-depletion fluorescence microscopy. *Opt. Lett.*, 19(11):780–782.
- Hohage, T. and Werner, F. (2016). Inverse problems with poisson data: statistical regularization theory, applications and algorithms. *Inverse Probl.*, 32:093001, 56.
- Holzmann, H., Bissantz, N., and Munk, A. (2007). Density testing in a contaminated sample. *J. Multivariate Anal.*, 98(1):57–75.

- Ingster, Y., Laurent, B., and Marteau, C. (2014). Signal detection for inverse problems in a multidimensional framework. *Math. Methods Statist.*, 23(4):279–305.
- Ingster, Y. I. (1993). Asymptotically minimax hypothesis testing for nonparametric alternatives. I-III. *Math. Methods Statist.*, 2:85–114, 171–189, 249–268.
- Ingster, Y. I., Sapatinas, T., and Suslina, I. A. (2012). Minimax signal detection in ill-posed inverse problems. *Ann. Statist.*, 40(3):1524–1549.
- Johnstone, I. M., Kerkyacharian, G., Picard, D., and Raimondo, M. (2004). Wavelet deconvolution in a periodic setting. *J. R. Stat. Soc. Ser. B Stat. Methodol.*, 66(3):547–573.
- Johnstone, I. M. and Paul, D. (2014). Adaptation in some linear inverse problems. *Stat*, 3(1):187–199.
- Johnstone, I. M. and Silverman, B. W. (1991). Discretization effects in statistical inverse problems. *J. Complexity*, 7:1–34.
- Kabluchko, Z. (2011). Extremes of the standardized Gaussian noise. *Stochastic Process. Appl.*, 121(3):515–533.
- Kazantsev, I., Lemahieu, I., Salov, G., and Denys, R. (2002). Statistical detection of defects in radiographic images in nondestructive testing. *Signal Processing*, 82(5):791 – 801.
- Kerkyacharian, G., Kyriazis, G., Le Pennec, E., Petrushev, P., and Picard, D. (2010). Inversion of noisy Radon transform by SVD based needlets. *Appl. Comput. Harmon. Anal.*, 28(1):24–45.
- Khoshnevisan, D. (2002). *Multiparameter Processes - An Introduction*. Springer, New York.
- Klar, T. A. and Hell, S. W. (1999). Subdiffraction resolution in far-field fluorescence microscopy. *Opt. Lett.*, 24(14):954–956.
- Komlós, J., Major, P., and Tusnády, G. (1975). An approximation of partial sums of independent RV's and the sample DF. I. *Z. Wahrscheinlichkeitstheorie und Verw. Gebiete*, 32:111–131.
- Laurent, B., Loubes, J.-M., and Marteau, C. (2011). Testing inverse problems: a direct or an indirect problem? *J. Statist. Plann. Inference*, 141(5):1849–1861.
- Laurent, B., Loubes, J.-M., and Marteau, C. (2012). Non asymptotic minimax rates of testing in signal detection with heterogeneous variances. *Electron. J. Stat.*, 6:91–122.
- Li, H., Munk, A., and Sieling, H. (2016). FDR-control in multiscale change-point segmentation. *Electron. J. Stat.*, 10(1):918–959.
- Mair, B. A. and Ruymgaart, F. H. (1996). Statistical inverse estimation in Hilbert scales. *SIAM J. Appl. Math.*, 56(5):1424–1444.
- Martean, C. and Mathé, P. (2014). General regularization schemes for signal detection in inverse problems. *Math. Methods Statist.*, 23(3):176–200.
- Mathé, P. and Pereverzev, S. V. (2002). Direct estimation of linear functionals from indirect noisy observations. *J. Complexity*, 18(2):500–516.
- Meister, A. (2009). *Deconvolution problems in nonparametric statistics*, volume 193 of *Lecture Notes in Statistics*. Springer-Verlag, Berlin.
- Nickl, R. and Reiß, M. (2012). A Donsker theorem for Lévy measures. *J. Funct. Anal.*, 263(10):3306–3332.
- O’Sullivan, F. (1986). A statistical perspective on ill-posed inverse problems. *Statist. Sci.*, 1(4):502–527. With comments and a rejoinder by the author.

- Pawley, J. E., editor (2006). *Handbook of Biological Confocal Microscopy*. Springer.
- Piterbarg, V. I. (1996). *Asymptotic methods in the theory of Gaussian processes and fields*, volume 148 of *Translations of Mathematical Monographs*. American Mathematical Society, Providence, RI. Translated from the Russian by V. V. Piterbarg, Revised by the author.
- Rio, E. (1993). Strong approximation for set-indexed partial-sum processes, via KMT constructions. II. *Ann. Probab.*, 21(3):1706–1727.
- Rohde, A. (2008). Adaptive goodness-of-fit tests based on signed ranks. *Ann. Statist.*, 36(3):1346–1374.
- Rufibach, K. and Walther, G. (2010). The block criterion for multiscale inference about a density, with applications to other multiscale problems. *J. Comput. Graph. Statist.*, 19(1):175–190. With supplementary data available online.
- Schmidt-Hieber, J., Munk, A., and Dümbgen, L. (2013). Multiscale methods for shape constraints in deconvolution: Confidence statements for qualitative features. *Ann. Statist.*, 41(3):1299–1328.
- Sharpnack, J. and Arias-Castro, E. (2016). Exact asymptotics for the scan statistic and fast alternatives. *Electron. J. Stat.*, 10(2):2641–2684.
- Siegmund, D. and Yakir, B. (2000). Tail probabilities for the null distribution of scanning statistics. *Bernoulli*, 6(2):191–213.
- Snyder, D. L., Helstrom, C. W., Lanterman, A. D., White, R. L., and Faisal, M. (1995). Compensation for readout noise in ccd images. *J. Opt. Soc. Am.*, 12(2):272–283.
- Snyder, D. L., White, R. L., and Hammoud, A. M. (1993). Image recovery from data acquired with a charge-coupled-device camera. *J. Opt. Soc. Am.*, 10(5):1014–1023.
- Söhl, J. and Trabs, M. (2012). A uniform central limit theorem and efficiency for deconvolution estimators. *Electron. J. Stat.*, 6:2486–2518.
- Sun, W., Reich, B. J., Cai, T. T., Guindani, M., and Schwartzman, A. (2015). False discovery control in large-scale spatial multiple testing. *J. R. Stat. Soc. Ser. B. Stat. Methodol.*, 77(1):59–83.
- Ta, H., Keller, J., Haltmeier, M., Saka, S. K., Schmied, J., Opazo, F., Tinnefeld, P., Munk, A., and Hell, S. W. (2015). Mapping molecules in scanning far-field fluorescence nanoscopy. *Nat. Commun.*, 6:7977.
- Tsybakov, A. (2000). On the best rate of adaptive estimation in some inverse problems. *C. R. Acad. Sci. Paris Sér. I Math.*, 330(9):835–840.
- van der Vaart, A. and Wellner, J. (1996). *Weak convergence and empirical processes. With applications to statistics*. Springer, New York.
- Walther, G. (2010). Optimal and fast detection of spatial clusters with scan statistics. *Ann. Statist.*, 38(2):1010–1033.
- Willer, T. (2009). Optimal bounds for inverse problems with Jacobi-type eigenfunctions. *Statist. Sinica*, 19(2):785–800.
- Zhang, N. R., Yakir, B., Xia, L. C., and Siegmund, D. (2016). Scan statistics on Poisson random fields with applications in genomics. *Ann. Appl. Stat.*, 10(2):726–755.